Ca^{2+} first enters the cytosol from the extracellular space through glutamate receptors, and then a large amount of Ca^{2+} is released from the ER to the cytosol (Paschen and Frandsen 2001; Hajnoczky *et al.* 2003). Disturbance of Ca^{2+} homeostasis in the ER leads to its dysfunction. Other conditions such as hypoxia, hypoglycaemia, and mutation of 'secretory' protein genes induce ER dysfunction and ER stress (Kaufman *et al.* 2002; Oyadomari *et al.* 2002a,b; Oyadomari and Mori 2004). When cells experience severe ER stress, the C/EBP homologous protein (CHOP), also known as growth arrest and DNA damage-inducible gene 153 (GADD 153), is induced in certain cell types (Ron and Habener 1992; Barone *et al.* 1994; Oyadomari *et al.* 2002a,b). CHOP is expressed at low levels under physiological conditions and is highly induced in response to ER stress (Ron *et al.* 1992). Induction of CHOP plays a key role in the pathway of ER stress-mediated apoptosis (Kawahara *et al.* 2001; Oyadomari *et al.* 2001; Gotoh *et al.* 2002; Oyadomari *et al.* 2002a,b; Gotoh *et al.* 2004; Oyadomari *et al.* 2004; Tajiri *et al.* 2004; Tsutsumi *et al.* 2004).

In this study, we report that CHOP is induced in cells of the GCL following NMDA treatment and that CHOP-deficient mice are more resistant to NMDA-induced retinal neuronal cell death.

Materials and methods

NMDA-induced retinal injury

All experiments conformed to the ARVO Statement for the Use of Animals in Ophthalmic and Vision Research. $CHOP^{-/-}$ mice (C57 BL/6 background) were provided by Dr Shizuo Akira (Osaka University, Japan). C57 BL/6 and $CHOP^{-/-}$ male mice, 8–12 weeks old, were used in this study. Mice were anaesthetized by intramuscular injection of 0.025 mg of ketamine hydrochloride (Sankyo, Tokyo, Japan) and 0.1 mg of xylazine (Bayer, Leverkusen, Germany). After the pupil was dilated with phenylephrine hydrochloride and tropicamide, injection into the vitreous cavity was performed under a microscope using a 33-gauge needle connected to a microsyringe and inserted toward to the posterior pole carefully, and not inserted too deep to avoid lens damage, approximately 1 mm behind the corneal limbus. NMDA and NMDA antagonst, MK-801 were obtained from Sigma (St Louis, MO, USA). A single dose of 2 mL of sterilized phosphate-buffered saline (PBS) containing NMDA was injected into the vitreous cavity. Some mice were systemically treated with 0.01 mg of MK-801 through a single injection into the peritoneal cavity 1 h before intravitreous NMDA injection. Control mice received either no injection or an injection of 2 mL of PBS into the vitreous cavity.

Real-time reverse transcription-polymerase chain reaction (RT-PCR) of CHOP mRNA

NMDA (5 nmol/2 mL) was injected into the vitreous cavity in C57 BL/6 mice. At 2, 6, 12 and 24 h after NMDA injection, mice were killed. At 2, 6 and 12 h, PBS-injected mice or NMDA-injected mice after pretreatment with MK-801(0.01 mg) were also killed. Eyes were dissected immediately, and total RNA was isolated from mouse retina using the AquaPure RNA isolation kit (Bio-Rad Laboratories, Hercules, CA, USA). To remove genomic DNA, the total RNA preparation was treated with deoxyribonuclease I (Invitrogen, Carlsbad, CA, USA). Assay-on-demand primers and probes systems (Applied Biosystems, Foster City, CA, USA) were used to quantify mRNAs for mouse CHOP Assay ID; Mm 00492097 and glyceraldehydes-3-phosphate dehydrogenase (GAPDH Assay ID; Mm 999999 15). These commercially available primers and probes sets, whose sequences were undocumented and whose PCR products were composed to be about 100 base pairs, were widely used (Staller *et al.* 2003; Tokuhiro *et al.* 2003; Roy *et al.* 2004). These primer sets were designed to span exon–exon junctions to eliminate any influence from the presence of contaminant genomic DNA. Real-time RT-PCR was performed with 10 ng of total RNA on an ABI Prism 7000 Sequence Detection System (Applied Biosystems) using the SuperScript One-Step RT-PCR system (Gibco BRL, Grand Island, NY, USA). Total RNA was reverse transcribed into cDNA using one cycle at 50°C for 30 min and one cycle at 95°C for 10 min cDNA was amplified using 40 cycles at 94°C for 15 s and 60°C for 1 min. Fluorescence changes of SYBR Green, the green fluorescent dye were monitored after each cycle. Melting curve analysis was performed (0.5°C/s increase from 55°C to 95°C with continuous fluorescence readings) at the end of 40 cycles to ensure that specific PCR products were obtained. The threshold cycle of fluorescence units was evaluated to quantify the amount of each mRNA level. Each CHOP mRNA level was normalized by the GAPDH mRNA level, and expressed as a mean ± standard deviation. The adjusted CHOP mRNAs after NMDA treatment were statistically analyzed using the ANOVA test. PCR products after 25 cycles for CHOP gene and 25 cycles for GAPDH gene were run by electrophoresis on a 1.5% agarose gel, to check size of PCR (and reaction specificity) and to confirm quantificative results of real-time RT-PCR.

Immunohistochemical staining

NMDA (5 nmol/2 mL) was injected into the vitreous cavity in C57 BL/6 mice. Mice were killed at 2, 6 and 12 h after NMDA injection. As control experiments, mice were treated with either intravitreous PBS injection or intravitreous NMDA injection after 0.01 mg of MK-801 pretreatment. The eyes were immediately enucleated and fixed with 4% paraformaldehyde in PBS. Specimens were dehydrated and embedded into paraffin. Transverse paraffin sections (3-mm thick), including the optic disc, were soaked in xylene, rehydrated in graded ethanols, and then washed with PBS. Sections were treated with 50 mg/mL trypsin and then washed three times. Each section was incubated for 30 min in PBS containing 2% horse serum and 5% skim milk to block non-specific binding. Monoclonal anti-mouse CHOP antibody (Santa Cruz Biotechnology, Santa Cruz, CA, USA) was used at a dilution of 1 : 200 in PBS containing 5% skim milk. Sections were incubated with this antibody overnight at 4°C and then washed three times in PBS. Sections were then incubated with mouse anti-mouse IgG HRP (horseradish peroxidase) antibody (Amersham, Buckinghamshire, UK) for 1 h at room temperature at a dilution of 1 : 500 in PBS. After washing with PBS three times, sections were amplified using the TSA (tyramide signal amplification) biotin system (PerkinElmer, Boston, MA, USA). They were incubated in the biotinyl tyramide

amplification reagent (Perkin Elmer) for 15 min at room temperature and washed with PBS three times. Following this, all slides were incubated with streptavidin Alexa Fluor 488 conjugate (Molecular Probes, Eugene, OR, USA) at a dilution of 1 : 500 in PBS for 30 min in the dark. After washing with PBS, sections were stained with propidium iodide (PI) for 15 min in the dark to illustrate retinal cell distribution and to clear retinal layers such as GCL, INL and outer nuclear layer. After washing with PBS, the number of CHOP-positive cells (in GCL and INL) and the number of PI stained cells (in GCL) were counted at 1.0–1.5 mm from the optic disc using a confocal microscope FV300 (Olympus, Tokyo, Japan), and expressed in millimetres. The percentage of the number of CHOP positive cells for that of PI stained cells was calculated in GCL of mouse retina. One section of each mouse eye was used for counting.

Immunoblot analysis

NMDA (5 nmol/2 mL) was injected into the vitreous cavity in C57 BL/6 mice. At 6 h after NMDA injection, mice were killed. As control experiments, PBS-injected mice or NMDA-injected mice after pretreatment of MK-801 (0.01 mg) were also killed. The retinal tissue was immediately isolated and lysed with lysis buffer containing 1% Nonidet P-40, 150 mM NaCl, 50 mM Tris-HCl (pH 7.4), 1 mM EDTA, 0.25% sodium deoxycholate, and a protease inhibitor tablet, Complete Mini (Roche Molecular Biochemicals, Mannheim, Germany). Lysates were subjected to sodium dodecyl sulfate – polyacrylamide gel electrophoresis (SDS–PAGE) using a 12% Tris-glycine gel (Invitrogen). Following electrophoresis, proteins were transferred to nitrocellulose membranes. Membranes were blocked for 30 min at room temperature using a blocking solution containing 5% skim milk powder and 0.1% Tween-20 in Tris-buffered saline (TBS; pH 7.4), and then incubated with monoclonal anti-mouse CHOP antibody overnight at 4°C diluted 1 : 100 in TBS or monoclonal anti-mouse β-actin antibody (Sigma) diluted 1 : 50000 in TBS for 60 min at room temperature. Membranes were then washed three times and incubated with mouse anti-mouse IgG HRP antibody (Amersham) for 30 min at room temperature at a dilution of 1 : 4000 in TBS. Membranes were washed three times, treated with an enhanced chemiluminescence (ECL) western blotting detection reagent (Amersham) and then exposed to X-ray film. The density of the signal was quantified using NIH (National Institutes of Health) Image 6.2 software and CHOP expression levels were normalized for β-actin. Results are expressed as a mean ± standard deviation for four independent experiments and analyzed statistically using the ANOVA test. An extract of mouse NIH3T3 cells treated with 1 mM thapsigargin (Sigma) for 6 h was used as positive control.

Terminal deoxyribonucleotidyl transferase (TdT)-mediated fluorescein-16-dUTP nick-end labelling (TUNEL) assay

To compare the number of TUNEL-positive cells in wild-type and $CHOP^{-/-}$ mice, a single dose of 2 mL PBS containing 1, 2, 5 or 10 nmol of NMDA was injected into the vitreous cavity. At 24 h after NMDA injection, mice were killed. Eyes were immediately enucleated and fixed with 4% paraformaldehyde in PBS. After specimens were dehydrated and embedded into paraffin, 5-mm thick transverse sections, including the optic disc, were cut. Sections were soaked in xylene to remove paraffin, rehydrated in graded ethanols, and then washed with PBS. The TUNEL assay was performed using the Apoptosis Detection System, Fluorescein (Promega, Madison, WI, USA) according to the manufacturer's protocol. The sections were stained with PI. The number of TUNEL-positive cells (in GCL and INL) and that of PI stained cells (in GCL) were counted at 1.0–1.5 mm from the optic disc under a confocal microscope FV300, and expressed in millimetres. The percentage of the number of TUNEL-positive cells for that of PI stained cells was calculated in the GCL of mouse retina. One section of each mouse eye was used for counting. Data were analyzed using the Student's *t*-test.

Morphometric analysis

Morphometric analysis was conducted as previously described (Inomata *et al.* 2003a,b). $CHOP^{-/-}$ mice and age-matched C57 BL/6 male mice were used in this analysis. Briefly, at 7 days after 2 nmol NMDA injection, mice were killed and eyes were enucleated. The eyes were immersed in 2.5% glutaraldehyde and 2% paraformaldehyde in PBS overnight at 4°C, followed by dehydration and paraffin embedding. Transverse sections 3 mm in thickness, including the optic disc, were prepared from the mouse eyes. Sections were stained with hematoxylin–eosin and photographed at 1.0 mm from the optic disc. The thickness of the inner plexiform layer, INL, outer plexiform layer, and outer nuclear layer was measured and shown as a mean ± standard deviation. The number of residual cells in the GCL (1.0–1.5 mm from the optic disc) was counted and expressed a mean ± standard deviation (in millimetres). One section of each mouse eye was used for counting. Data were analyzed using the Student's *t*-test.

Results

Real-time RT-PCR analysis using total RNA derived from mouse retina was performed to quantify CHOP mRNA expression following NMDA injection (Fig. 1). At 2 h after NMDA treatment, the relative expression level of CHOP mRNA increased to 316 ± 116% of the basal level ($p = 0.005$; 0 vs. 2 h, $p = 0.010$; 2 vs. 24 h, ANOVA). It then decreased to 220 ± 126, 219 ± 116, and 121 ± 68%, at 6, 12 and 24 h after NMDA injection, respectively. After PBS injection, the relative expression level of CHOP mRNA significantly increased to 179 ± 74% of the basal level ($p = 0.010$; 0 vs. 2 h, $p = 0.007$; 2 vs. 6 h, $p = 0.004$; 2 vs. 12 h, ANOVA). After then it was decreased to almost basal level. Similarly, it was significantly increased at 2 h after NMDA treatment in the eyes with pretreatment with MK-801 ($p = 0.007$; 0 vs. 2 h, $p = 0.002$; 2 vs. 6 h, $p = 0.0002$; 2 vs. 12 h, ANOVA). After then, it was decreased to almost basal level. By TUNEL staining assay, TUNEL-positive cells appeared in GCL and INL after 6 h, and then increased up to 24 h after NMDA treatment. However, TUNEL-positive cells were undetectable at any time points (2, 6, 12, 24 h) either in the eyes injected with PBS or in the eyes injected with NMDA after systemic MK-801 pretreatment (data not shown).

In our immunohistochemical analysis, immunoreactivity for CHOP was not conspicuous in the mouse retina under normal conditions (Fig. 2). At 2 h after NMDA injection,

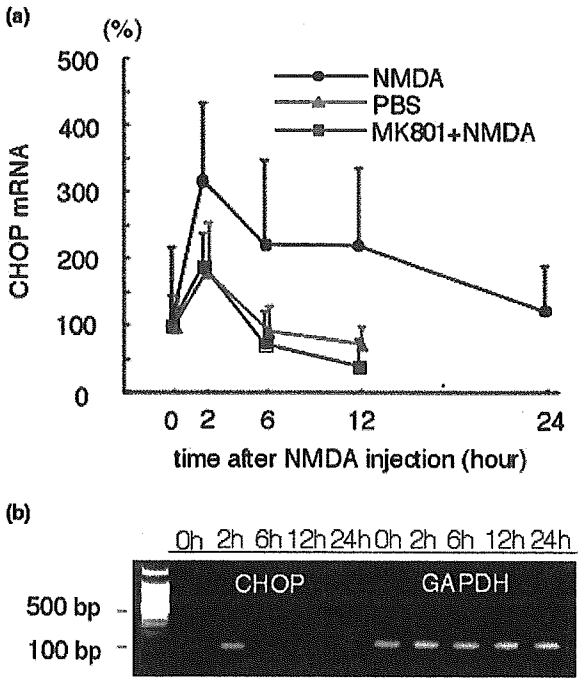

Fig. 1 Expression of CHOP mRNA in mouse retina following NMDA treatment. (a) Real-time RT-PCR analysis of CHOP mRNA was performed after intravitreous NMDA (black) or PBS (green) injection. Some mice were systemically pretreated with MK-801 before intravitreous NMDA injection (red). CHOP mRNA was standardized with GAPDH mRNA. CHOP mRNA was set at 100% in control and expressed as a mean ± standard deviation ($n = 5$–8). Data were analyzed using the ANOVA test. Asterisks indicate statistically significant differences. (b) RT-PCR experiment of CHOP mRNA and GAPDH mRNA after NMDA injection is shown.

CHOP immunoreactivity was found in cells present in the GCL, and the mean number of CHOP-positive cells in the GCL increased to 6.1 ± 5.6 cells/mm ($p = 0.037$; 0 vs. 2 h, ANOVA). At 6 h after NMDA treatment, CHOP-positive cells significantly increased to 30.9 ± 1.8 cells/mm in the GCL ($p < 0.0001$; 0 vs. 6 h, 2 vs. 6 h, 6 vs. 12 h, ANOVA). At 12 h after NMDA treatment, the number of CHOP-positive cells decreased to near basal levels (0.6 ± 1.1 cells/mm). In contrast, no CHOP-positive cells were found in control experiments at any time points either with intravitreous injection of PBS or with intravitreous injection of NMDA after systemic MK-801 pretreatment. Additionally, an immunoblot assay was performed to evaluate the relative expression level of CHOP protein (Fig. 3). Under normal conditions, CHOP protein was faintly detected in immunoblot experiments of mouse retinal samples. In both PBS-injected eyes and NMDA-injected eyes after pretreatment with MK-801, the expression level for CHOP protein was almost the same level as that in the untreated eye. After NMDA injection, the relative expression level of CHOP increased to 178 ± 21% of basal levels ($p = 0.001$; no treatment vs. NMDA, $p = 0.0005$; PBS vs. NMDA, ANOVA).

The TUNEL assay was performed in the mouse retina of the two strains 24 h after NMDA treatment (Fig. 4). In control experiments using PBS injection, no TUNEL-positive cells were found in C57 BL/6 and CHOP$^{-/-}$ mice. Furthermore, following intravitreous injection of 1 nmol NMDA, only a small number of TUNEL-positive cells were found in the retina of C57 BL/6 and CHOP$^{-/-}$ mice. However, following injection of 2 nmol NMDA, the mean number of TUNEL-positive cells in the GCL of CHOP$^{-/-}$ mice (6.8 ± 3.8 cells/mm) were significantly lower than that of C57 BL/6 mice (18.8 ± 7.4 cells/mm, $p = 0.025$, Student's *t*-test). Similarly, the percentage of CHOP positive cells for TUNEL-stained cells in the GCL of CHOP$^{-/-}$ mice (6.4 ± 3.7%) was significantly lower than that of C57 BL/6 mice (16.8 ± 4.9%, $p = 0.001$, Student's *t*-test). Furthermore, the number of TUNEL-positive cells in the INL of CHOP$^{-/-}$ mice (5.0 ± 3.7 cells/mm) was significantly lower than the number in C57 BL/6 mice (19.8 ± 4.6 cells/mm, $p = 0.001$, Student's *t*-test). After injection of 5 nmol NMDA, the mean number of TUNEL-positive cells in the GCL of CHOP$^{-/-}$ mice (15.3 ± 13.1 cells/mm) was significantly lower than the number in C57 BL/6 mice (36.3 ± 7.5 cells/mm, $p = 0.036$, Student's *t*-test). Similarly, the percentage of CHOP-positive cells to TUNEL-stained cells in the GCL of CHOP$^{-/-}$ mice (18.1 ± 14.9%) was significantly lower than that of C57 BL/6 mice (48.9 ± 6.3%, $p = 0.001$, Student's *t*-test). However, there was no significant difference in the number of TUNEL-positive cells in the INL of CHOP$^{-/-}$ (37.3 ± 19.3 cells/mm) and C57 BL/6 (44.3 ± 8.2 cells/mm) mice. Additionally, in experiments using a large amount of NMDA (10 nmol), no statistically significant difference was found in either the GCL or INL of these two strains.

Morphological changes were then measured in experiments employing two strains (C57 BL/6 and CHOP$^{-/-}$) following intravitreal injection of 2 nmol NMDA (Fig. 5). In both C57 BL/6 and CHOP$^{-/-}$ mice, the thickness of the inner plexiform layer and INL decreased significantly following NMDA injection. The mean thickness of the IPL in CHOP$^{-/-}$ and in C57 BL/6 mice was 20.3 ± 5.4 and 14.7 ± 4.2 mm, respectively, showing a significant difference ($p = 0.018$, Student's *t*-test). Similarly, the mean thickness of the INL in CHOP$^{-/-}$ and in C57 BL/6 mice was 22.7 ± 4.8 and 18.5 ± 3.5 mm, respectively ($p = 0.040$, Student's *t*-test). Additionally, in experiments with NMDA treatment, the number of cells in the GCL of CHOP$^{-/-}$ mice was 34.8 ± 11.4 cells/mm, which was higher than that in C57 BL/6 mice (24.1 ± 7.7 cells/mm, $p = 0.026$, Student's *t*-test). In contrast, in the outer retinal layers such as the outer plexiform and outer nuclear layers, no difference was observed. Furthermore, in control experiments using intravitreous PBS injection, there was no significant difference in the thickness of any retinal layers of C57 BL/6 and CHOP$^{-/-}$ mice.

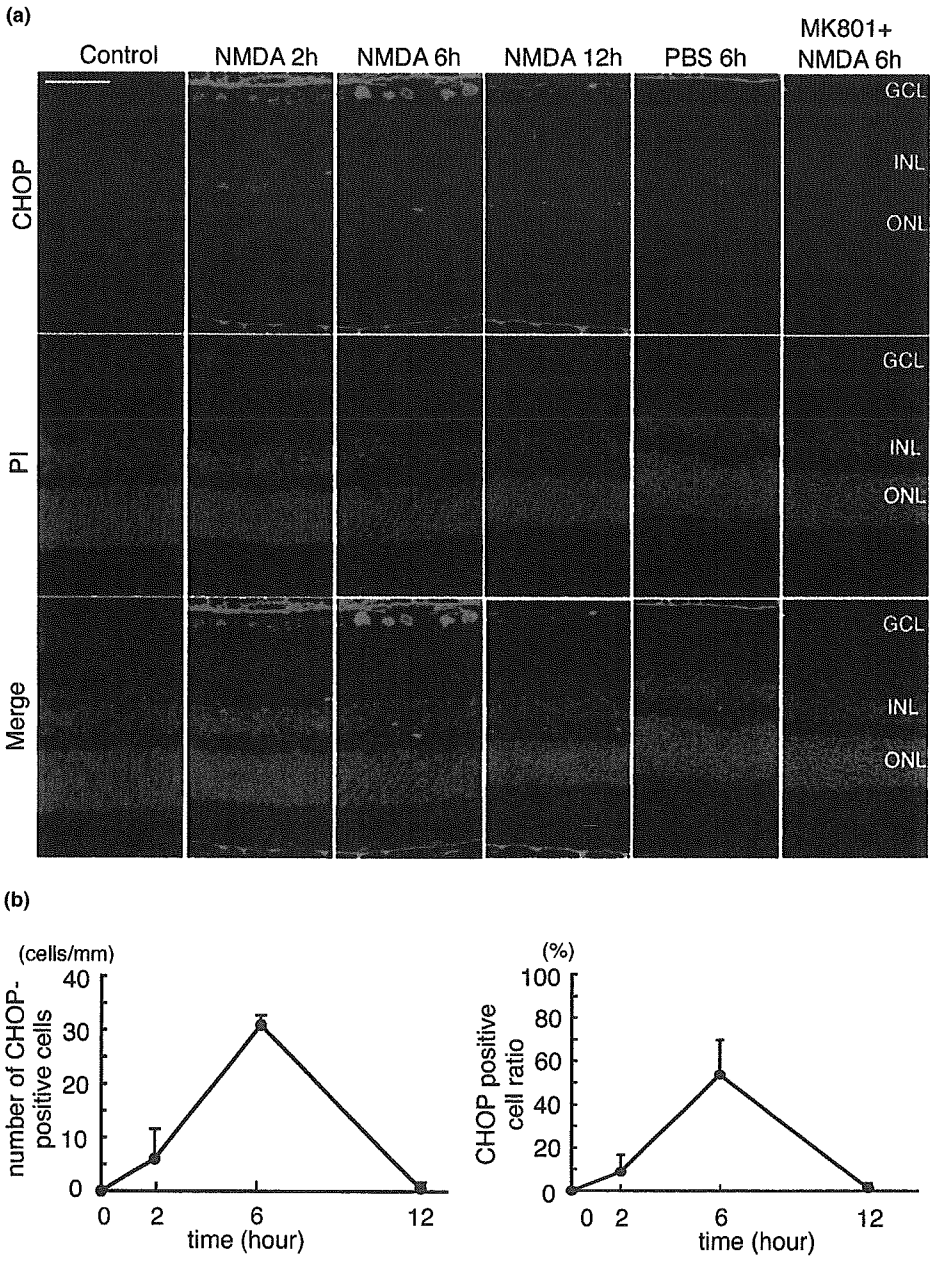

Fig. 2 Immunohistochemical analysis for CHOP protein in mouse retina following NMDA treatment. (a) Immunohistochemical analysis was performed in the eyes with NMDA injection, PBS injection, or NMDA injection after systemic MK-801 treatment. Propidium iodide (PI) staining was also performed. GCL, ganglion cell layer; INL, inner nuclear layer; ONL, outer nuclear layer. Scale bar: 50 mm. (b) The number of CHOP-positive cells was counted and shown as a mean ± standard deviation ($n = 3$). The ratio of CHOP-positive cells/PI stained cells was also shown.

Discussion

In a number of visual-threatening ocular diseases such as ischaemic retinal disease and glaucoma, glutamate toxicity has been regarded as one of the major mechanisms related to retinal neuronal cell death (Kuroiwa *et al.* 1998; Dkhissi *et al.* 1999; Lam *et al.* 1999a,b). This hypothesis is supported by the fact that glutamate receptor antagonists show a neuroprotective effect against some forms of retinal injury and ocular hypertension (glaucoma) in animal experiments (Rosner *et al.* 1997; Chaudhary *et al.* 1998; Sun *et al.* 2001). Recently, notions pertaining to the involvement of ER stress

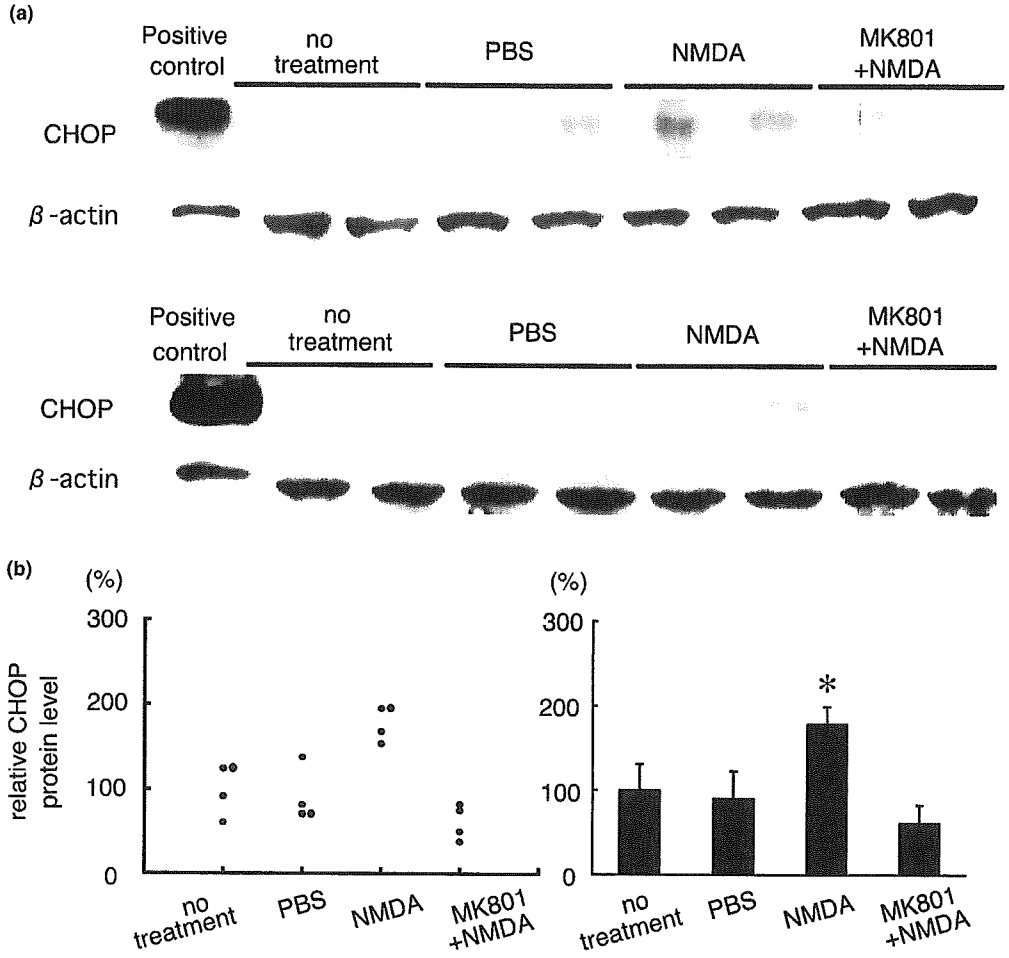

Fig. 3 Immunoblot analysis of CHOP protein following NMDA injection. (a) The homogenates from the retina with no injection, PBS injection, NMDA injection, or NMDA injection after MK-801 pretreatment were subjected to immunoblot analysis. The homogenate from NIH3T3 cells treated with 1 mM thapsigargin was used as a positive control. (b) The amount of CHOP protein was quantified by densitometric analysis and standardized for β-actin. The average of CHOP protein in the retina with no treatment was set at 100%. Data ($n = 4$) were indicated as dot in the left graph. Data are shown as a mean ± standard deviation in the right graph. Data were analyzed using the ANOVA test. Asterisks indicate statistically significant differences.

in neuronal damage have received much attention by investigators. The molecular mechanisms involved have been shown to play an important role in neurodegenerative disorders such as Alzheimer's disease (Mattson and Chan 2003; Katayama *et al.* 2004; Pereira *et al.* 2004), Parkinson's disease (Imai *et al.* 2000; Chen *et al.* 2004), polyglutamine diseases (Kouroku *et al.* 2002; Nishitoh *et al.* 2002; Takeda *et al.* 2002), and brain ischaemia (DeGracia and Montie 2004; Kitano *et al.* 2004). To date, however, there has been no investigation concerning the involvement of ER stress in the pathogenesis of retinal injury (or glaucoma). Among the ER stress-related molecules, CHOP is known to be highly induced in response to ER stress and is implicated to play a role in apoptosis (Ron *et al.* 1992). Induction of this molecule is thought to play an important role in the pathway of ER stress-mediated apoptosis (Kawahara *et al.* 2001; Oyadomari *et al.* 2001; Gotoh *et al.* 2002; Oyadomari *et al.* 2002a,b; Gotoh *et al.* 2004; Oyadomari *et al.* 2004; Tajiri *et al.* 2004; Tsutsumi *et al.* 2004). A previous report of gene-array analysis on NMDA-induced retinal injury showed an up-regulation of some molecules, including a 3.7-fold increase in CHOP (Laabich *et al.* 2001). This exhaustive assay, using microarray, already predicted the importance of the CHOP gene in NMDA retinal injury. In the present study, we clearly showed the important role of the CHOP gene in neuronal cell death in NMDA-induced retinal damage.

Our results from a series of experiments showed that CHOP is up-regulated in eyes with NMDA-induced retinal injury. Real-time RT-PCR experiments showed that the relative level of CHOP mRNA expression peaked at 2 h after

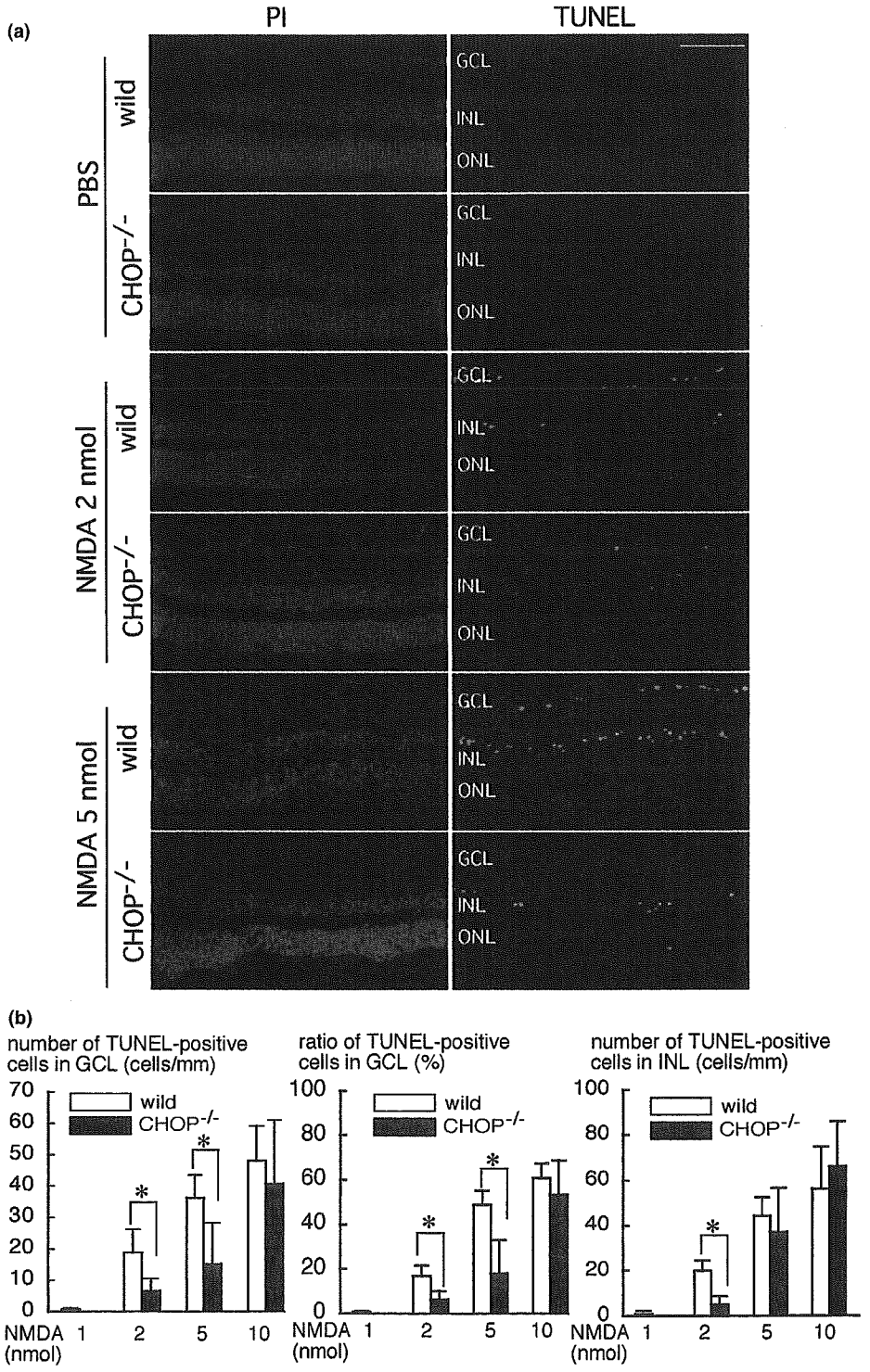

Fig. 4 (a) Terminal deoxyribonucleotidyl transferase (TdT)- mediated fluorescein-16-dUTP nick-end labelling (TUNEL) staining of wild-type and CHOP$^{-/-}$ mouse retina at 24 h after NMDA treatment. Propidium iodide (PI) staining was also performed. Scale bar: 50 mm. GCL, ganglion cell layer; INL, inner nuclear layer; ONL, outer nuclear layer. (b) The number of TUNEL-positive cells in GCL and that in INL were counted and expressed as a mean ± standard deviation ($n = 4$–6). The ratio of TUNEL-positive cells/PI stained cells was calculated and shown. Data were analyzed using the Student's *t*-test.

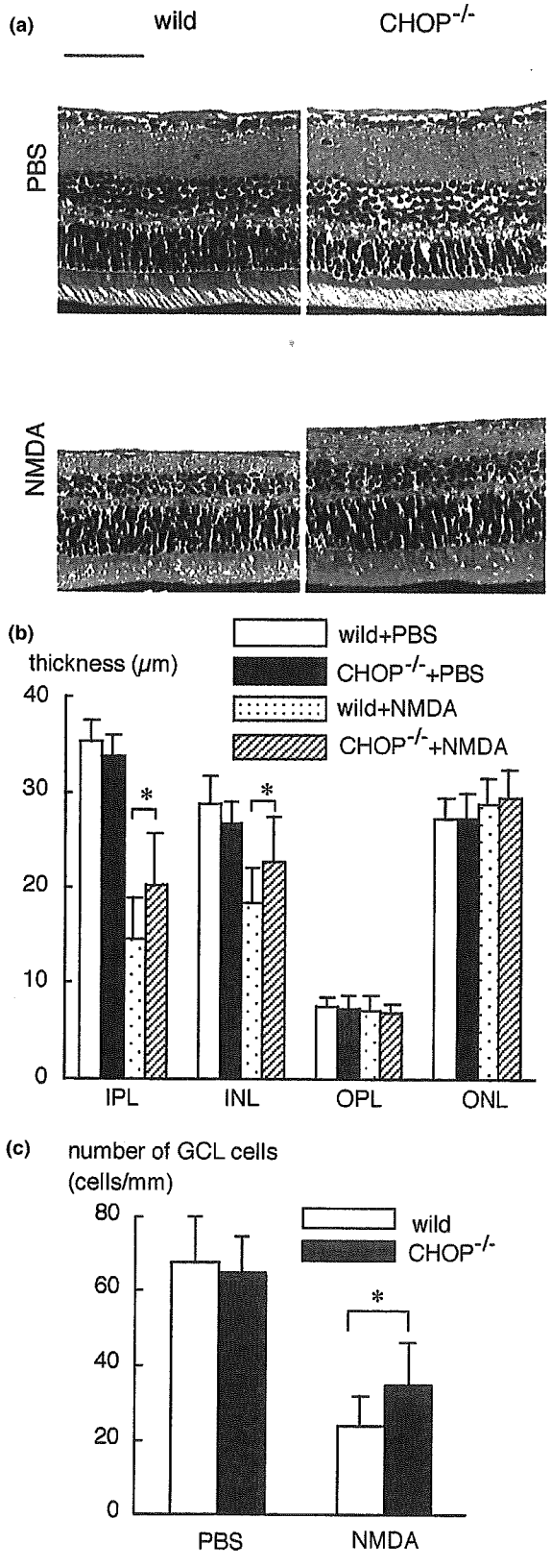

Fig. 5 Morphological analysis of wild-type and CHOP$^{-/-}$ mouse retina at 7 days after 2 nmol NMDA treatment. (a) Paraffin sections stained with hematoxylin-eosin. GCL, ganglion cell layer; IPL, inner plexiform layer; INL, inner nuclear layer; OPL, outer plexiform layer; ONL, outer nuclear layer; PR, photoreceptor. (b) The thickness of retinal layers such as IPL, INL, OPL and ONL was measured and shown as a mean ± standard deviation ($n = 10$). Data were analyzed using the Student's *t*-test. Scale bar: 50 mm. (c) The number of residual cells in the ganglion cell layer was counted and shown as a mean ± standard deviation. Data were analyzed using the Student's *t*-test.

NMDA injection. Given that CHOP immunoreactivity in retinal sections of the GCL peaked at 6 h after NMDA treatment, up-regulated expression of the CHOP protein can be expected to follow the increased expression of CHOP mRNA. However, in either of the eyes with PBS injection or those with NMDA injection after MK-801 treatment, mRNA for CHOP was induced in our real-time RT-PCR study, but CHOP protein induction was not observed in our immunohistochemical and immunoblot studies. It seemed that inductions of CHOP protein in these control eyes were under the detection limits of our assays. All these results may imply a contribution of CHOP to the onset and progression of apoptotic cell death in retinal tissue caused by NMDA, as TUNEL-positive cells appeared after 6 h, and then increased during the following 24 h after NMDA treatment.

It was somewhat surprising that CHOP protein was induced strongly in retinal cells of the GCL but little expressed in retinal cells of INL, although TUNEL-positive cells were observed in both the GCL and INL. A number of retinal ganglion cells are located in the GCL, and apoptosis of these cells plays a key role in the pathogenesis of glaucoma, a major cause of blindness (Quigley *et al.* 1995; Rosenbaum *et al.* 1998). It was known that susceptibility for ER stress differs markedly from cell to cell, and organ to organ. The pancreatic β-cell, having abundant ER in the cytoplasm and synthesizing insulin vigorously, is one of the most susceptible cells for ER stress (Oyadomari *et al.* 2001). Ultrastructural observations have demonstrated that the cytoplasm of retinal ganglion cells contains abundant ER, suggesting active synthesis of 'secretary' proteins (Sigelman *et al.* 1982). Retinal ganglion cells might be more susceptible to ER stress than other retinal cells in INL. Our observation of increased expression of CHOP protein in retinal cells of GCL may be associated with these cell characteristics of retinal ganglion cells.

ER functions as an intracellular calcium store and plays an important role in Ca^{2+} homeostasis by pumping Ca^{2+} via the ER rumen (Paschen 2003). NMDA caused Ca^{2+} influx from the ER to cytosol, and resulted in ER Ca^{2+} depletion and ER stress (Paschen *et al.* 2001). ER stress followed by Ca^{2+} depletion induces the CHOP gene (Oyadomari *et al.* 2004). In our report, overexpression of calreticulin, a major binding protein in ER, increases ER Ca^{2+} stores and protects against

nitric oxide-induced (CHOP-mediated) apoptosis (Oyadomari *et al.* 2001). As mentioned above, it was thought that NMDA depletes ER Ca^{2+} stores, leads ER dysfunction and CHOP protein induction in retinal cells in the GCL. However, the precise apoptosis cascade downstream of CHOP is not well known. It was reported that overexpression of Bcl-2 blocked CHOP-induced apoptosis (Matsumoto *et al.* 1996) and overexpression of CHOP leads to a decrease in Bcl-2 protein (McCullough *et al.* 2001). We recently found that CHOP-induced apoptosis in RAW 264.7 macrophages is mediated by translocation of Bax from the cytosol to the mitochondria (Gotoh *et al.* 2004). Further study is required to reveal in detail the cascade of CHOP downstream.

Morphological abnormality was not seen in adult ocular tissues of $CHOP^{-/-}$ mice. $CHOP^{-/-}$ mice were reported to display normal development and fertility (Zinszner *et al.* 1998; Oyadomari *et al.* 2001). Similarly, normal development and fertility was reported in other ER stress-related gene knockout mice, such as caspase $12^{-/-}$ mice and ASK1 (apoptosis signal-regulating kinase)$^{-/-}$ mice (Nakagawa *et al.* 2000; Tobiume *et al.* 2001). Therefore, knockout of the CHOP gene would probably not cause serious developmental abnormalities, because this gene might not have such an important role in ocular development. However, our present study demonstrated that $CHOP^{-/-}$ mice are more resistant to retinal injury when the injury was caused with low doses (2–5 nmol) of NMDA. Our results showed that the neuroprotective effects in CHOP-deficient mice against NMDA-induced retinal injury were limited. We speculate that other CHOP-independent apoptosis cascades, such as oxidative stress and DNA damage, might cause neuronal cell death in $CHOP^{-/-}$ mice. In the experiments using pancreatic b-cells, low doses of nitric oxide depleted ER Ca^{2+}, led to ER dysfunction, induced CHOP protein, and resulted in apoptosis. As the dose of nitric oxide was increased, other apoptosis molecules, such as DNA damage-related protein p53, were induced in addition to CHOP protein (Oyadomari *et al.* 2001). In addition, in $CHOP^{-/-}$ mice, pancreatic b-cells were more resistant to nitric oxide-induced apoptosis than those from wild-type mice (Oyadomari *et al.* 2001). Targeted disruption of the CHOP gene could delay b-cell apoptosis and diabetes mellitus in insulin 2 mutation diabetes mice (Oyadomari *et al.* 2002a). Furthermore, $CHOP^{-/-}$ mice were more resistant to neuronal cell death in brain ischaemia (Tajiri *et al.* 2004). However, unlike $CHOP^{-/-}$ mice, pancreatic islets derived from $CHOP^{+/-}$ mice were not resistant to nitric oxide-induced apoptosis (Oyadomari *et al.* 2001), and $CHOP^{+/-}$ mice could not block or delay the development of diabetes caused by insulin mutation (Oyadomari *et al.* 2002a).

In conclusion, our results indicated that intravitreous NMDA injection induced CHOP expression and led to apoptosis in the GCL. Disruption of the CHOP gene gave resistance to NMDA-induced retinal damage. We propose that the ER stress–CHOP pathway is a potential target that may prevent retinal neuronal cell apoptosis induced by excitatory amino acids.

Acknowledgements

We thank Shizuo Akira (Osaka University) for providing the $CHOP^{-/-}$ mice. This work was supported in part by a Grant-in-Aid for Scientific Research from the Ministry of Education, Science, Sports and Culture, Japan and from the Ministry of Health and Welfare, Japan. Commercial relationship policy: N.

References

Alberts B., Johnson A., Lewis J., Raff M., Roberts K. and Walter P. (2002) The endoplasmic reticulum, in *Molecular Biology of the Cell*, 4th edn. pp. 689–709. Garland Science, New York.

Barone M. V., Crozat A., Tabaee A., Philipson L. and Ron D. (1994) CHOP(GADD153) and its oncogenic variant, TLS-CHOP, have opposing effects on the induction of G1/S arrest. *Genes Dev.* **8**, 453–464.

Chaudhary P., Ahmed F. and Sharma S. C. (1998) MK801-a neuroprotectant in rat hypertensive eyes. *Brain Res.* **792**, 154–158.

Chen G., Bower K. A., Ma C., Fang S., Thiele C. J. and Luo J. (2004) Glycogen synthase kinase 3 (GSK3b) mediates 6-hydroxydopamine-induced neuronal death. *FASEB J.* **18**, 1162–1164.

DeGracia D. J. and Montie H. L. (2004) Cerebral ischemia and the unfolded protein response. *J. Neurochem.* **91**, 1–8.

Dkhissi O., Chanut E., Wasowicz M., Savoldelli M., Nguyen-Legros J., Minvielle F. and Versaux-Botteri C. (1999) Retinal TUNEL-positive cells and high glutamate levels in vitreous humor of mutant quail with a glaucoma-like disorder. *Invest. Ophthalmol. Vis. Sci.* **40**, 990–995.

Farrar G. J., Kenna P. F. and Humphries P. (2002) On the genetics of retinitis pigmentosa and on mutation-independent approaches to therapeutic intervention. *EMBO J.* **21**, 857–864.

Gotoh T., Oyadomari S., Mori K. and Mori M. (2002) Nitric oxide-induced apoptosis in RAW 264.7 macrophages is mediated by endoplasmic reticulum stress pathway involving ATF6 and CHOP. *J. Biol. Chem.* **277**, 12 343–12 350.

Gotoh T., Terada K., Oyadomari S. and Mori M. (2004) Hsp70-DnaJ chaperone pair prevents nitric oxide- and CHOP-induced apoptosis by inhibiting translocation of Bax to mitochondria. *Cell Death Differ.* **11**, 390–402.

Hajnoczky G., Davies E. and Madesh M. (2003) Calcium signaling and apoptosis. *Biochem. Biophys. Res. Commun.* **304**, 445–454.

Imai Y., Soda M. and Takahashi R. (2000) Parkin suppresses unfolded protein stress-induced cell death through its E3 ubiquitin-protein ligase activity. *J. Biol. Chem.* **275**, 35 661–35 664.

Inomata Y., Hirata A., Yonemura N., Koga T., Kido N. and Tanihara H. (2003a) Neuroprotective effects of interleukin-6 on NMDA-induced rat retinal damage. *Biochem. Biophys. Res. Commun.* **302**, 226–232.

Inomata Y., Hirata A., Koga T., Kimura A., Singh D. P., Shinohara T. and Tanihara H. (2003b) Lens epithelium-derived growth factor: neuroprotection on rat retinal damage induced by *N*-methyl-D-aspartate. *Brain Res.* **991**, 163–170.

Joo C. K., Choi J. S., Ko H. W., Park K. Y., Sohn S., Chun M. H., Oh Y. J. and Gwag B. J. (1999) Necrosis and apoptosis after retinal ischemia: involvement of NMDA-mediated excitotoxicity and p53. *Invest. Ophthalmol. Vis. Sci.* **40**, 713–720.

Katayama T., Imaizumi K., Manabe T., Hitomi J., Kudo T. and Tohyama M. (2004) Induction of neuronal death by ER stress in Alzheimer's disease. *J. Chem. Neuroanat.* **28**, 67–78.

Kaufman R. J., Scheuner D., Schroder M., Shen X., Lee K., Liu C. Y. and Arnold S. M. (2002) The unfolded protein response in nutrient sensing and differentiation. *Nat. Rev. Mol. Cell Biol.* **3**, 411–421.

Kawahara K., Oyadomari S., Gotoh T., Kohsaka S., Nakayama H. and Mori M. (2001) Induction of CHOP and apoptosis by nitric oxide in p53-deficient microglial cells. *FEBS Lett.* **506**, 135–139.

Kerrigan L. A., Zack D. J., Quigley H. A., Smith S. D. and Pease M. E. (1997) TUNEL-positive ganglion cells in human primary open-angle glaucoma. *Arch. Ophthalmol.* **115**, 1031–1035.

Kitano H., Nishimura H., Tachibana H., Yoshikawa H. and Matsuyama T. (2004) ORP150 ameliorates ischemia/reperfusion injury from middle cerebral artery occlusion in mouse brain. *Brain Res.* **1015**, 122–128.

Kouroku Y., Fujita E., Jimbo A. *et al.* (2002) Polyglutamine aggregates stimulate ER stress signals and caspase-12 activation. *Hum. Mol. Genet.* **11**, 1505–1515.

Kuroiwa S., Katai N., Shibuki H., Kurokawa T., Umihira J., Nikaido T., Kametani K. and Yoshimura N. (1998) Expression of cell cycle-related genes in dying cells in retinal ischemic injury. *Invest. Ophthalmol. Vis. Sci.* **39**, 610–617.

Laabich A., Li G. and Cooper N. G. (2001) Characterization of apoptosis-genes associated with. NMDA mediated cell death in the adult rat retina. *Brain Res. Mol. Brain Res.* **91**, 34–42.

Lam T. T., Abler A. S., Kwong J. M. and Tso M. O. (1999a) *N*-methyl-D-aspartate (NMDA)-induced apoptosis in rat retina. *Invest. Ophthalmol. Vis. Sci.* **40**, 2391–2397.

Lam T. T., Abler A. S. and Tso M. O. (1999b) Apoptosis and caspases after ischemia-reperfusion injury in rat retina. *Invest. Ophthalmol. Vis. Sci.* **40**, 967–975.

Matsumoto M., Minami M., Takeda K., Sakao Y. and Akira S. (1996) Ectopic expression of CHOP (GADD153) induces apoptosis in M1 myeloblastic leukemia cells. *FEBS Lett.* **395**, 143–147.

Mattson M. P. and Chan S. L. (2003) Neuronal and glial calcium signaling in Alzheimer's disease. *Cell Calcium* **34**, 385–397.

McCullough K. D., Martindale J. L., Klotz L. O., Aw T. Y. and Holbrook N. J. (2001) Gadd 153 sensitizes cells to endoplasmic reticulum stress by down-regulating Bcl2 and perturbing the cellular redox state. *Mol. Cell Biol.* **21**, 1249–1259.

Nakagawa T., Zhu H., Morishima N., Li E., Xu J., Yankner B. A. and Yuan J. (2000) Caspase-12 mediates endoplasmic-reticulum-specific apoptosis and cytotoxicity by amyloid-β. *Nature* **403**, 98–103.

Nishitoh H., Matsuzawa A., Tobiume K., Saegusa K., Takeda K., Inoue K., Hori S., Kakizuka A. and Ichijo H. (2002) ASK1 is essential for endoplasmic reticulum stress-induced neuronal cell death triggered by expanded polyglutamine repeats. *Genes Dev.* **16**, 1345–1355.

Oyadomari S. and Mori M. (2004) Roles of CHOP/GADD153 in endoplasmic reticulum stress. *Cell Death Differ.* **11**, 381–389.

Oyadomari S., Takeda K., Takiguchi M., Gotoh T., Matsumoto M., Wada I., Akira S., Araki E. and and. Mori M. (2001) Nitric oxide-induced apoptosis in pancreatic β cells is mediated by the endoplasmic reticulum stress pathway. *Proc. Natl Acad. Sci. USA* **98**, 10 845–10 850.

Oyadomari S., Koizumi A., Takeda K., Gotoh T., Akira S., Araki E. and Mori M. (2002a) Targeted disruption of the Chop gene delays endoplasmic reticulum stress-mediated diabetes. *J. Clin. Invest.* **109**, 525–532.

Oyadomari S., Araki E. and Mori M. (2002b) Endoplasmic reticulum stress-mediated apoptosis in pancreatic b-cells. *Apoptosis* **7**, 335–345.

Paschen W. (2003) Endoplasmic reticulum: a primary target in various acute disorders and degenerative diseases of the brain. *Cell Calcium* **34**, 365–383.

Paschen W. and Frandsen A. (2001) Endoplasmic reticulum dysfunction – a common denominator for cell injury in acute and degenerative diseases of the brain? *J. Neurochem.* **79**, 719–725.

Pereira C., Ferreiro E., Cardoso S. M. and de Oliveira C. R. (2004) Cell degeneration induced by amyloid-b peptides: implications for Alzheimer's disease. *J. Mol. Neurosci.* **23**, 97–104.

Quigley H. A., Nickells R. W., Kerrigan L. A., Pease M. E., Thibault D. J. and Zack D. J. (1995) Retinal ganglion cell death in experimental glaucoma and after axotomy occurs by apoptosis. *Invest. Ophthalmol. Vis. Sci.* **36**, 774–786.

Reme C. E., Grimm C., Hafezi F., Marti A. and Wenzel A. (1998) Apoptotic cell death in retinal degenerations. *Prog. Retin. Eye Res.* **17**, 443–464.

Ron D. and Habener J. F. (1992) CHOP, a novel developmentally regulated nuclear protein that dimerizes with transcription factors C/EBP and LAP and functions as a dominant-negative inhibitor of gene transcription. *Genes Dev.* **6**, 439–453.

Rosenbaum D. M., Rosenbaum P. S., Gupta H., Singh M., Aggarwal A., Hall D. H., Roth S. and Kessler J. A. (1998) The role of the p53 protein in the selective vulnerability of the inner retina to transient ischemia. *Invest. Ophthalmol. Vis. Sci.* **39**, 2132–2139.

Rosner M., Solberg Y., Turetz J. and Belkin M. (1997) Neuroprotective therapy for argon-laser induced retinal injury. *Exp. Eye Res.* **65**, 485–495.

Roy N. S., Nakano T., Keyoung H. M. *et al.* (2004) Telomerase immortalization of neuronally restricted progenitor cells derived from the human fetal spinal cord. *Nat. Biotechnol.* **22**, 297–305.

Sigelman J. and Ozanics V. (1982) Retina, in *Ocular Anatomy, Embryology, and Teratology* (Jakobiec, F. A., ed.), pp. 478–481. Harper and Row, Philadelphia.

Staller P., Sulitkova J., Lisztwan J., Moch H., Oakeley E. J. and Krek W. (2003) Chemokine receptor CXCR4 downregulated by von Hippel-Lindau tumour suppressor pVHL. *Nature* **425**, 307–311.

Sun Q., Ooi V. E. and Chan S. O. (2001) *N*-methyl-D-aspartate-induced excitotoxicity in adult rat retina is antagonized by single systemic injection of MK-801. *Exp. Brain Res.* **138**, 37–45.

Tajiri S., Oyadomari S., Yano S., Morioka M., Gotoh T., Hamada J. I., Ushio Y. and Mori M. (2004) Ischemia-induced neuronal cell death is mediated by the endoplasmic reticulum stress pathway involving CHOP. *Cell Death Differ.* **11**, 403–415.

Takeda K., Matsuzawa A., Nishitoh H., Tobiume K., Kishida S., Ninomiya-Tsuji J., Matsumoto K. and Ichijo H. (2002) ASK1 is essential for endoplasmic reticulum stress-induced neuronal cell death triggered by expanded polyglutamine repeats. *Genes Dev.* **16**, 1345–1355.

Tobiume K., Matsuzawa A., Takahashi T. *et al.* (2001) ASK1 is required for sustained activations of JNK/p38 MAP kinases and apoptosis. *EMBO Report* **2**, 222–228.

Tokuhiro S., Yamada R., Chang X. *et al.* (2003) An intronic SNP in a RUNX1 binding site of. SLC22A4, encoding an organic cation transporter, is associated with rheumatoid arthritis. *Nat. Genet.* **35**, 341–348.

Tsutsumi S., Gotoh T., Tomisato W. *et al.* (2004) Endoplasmic reticulum stress response is involved in nonsteroidal anti-inflammatory drug-induced apoptosis. *Cell Death Differ.* **11**, 1009–1016.

Wax M. B., Tezel G. and Edward P. D. (1998) Clinical and ocular histopathological findings in a patient with normal-pressure glaucoma. *Arch. Ophthalmol.* **116**, 993–1001.

Zinszner H., Kuroda M., Wang X., Batchvarova N., Lightfoot R. T., Remotti H., Stevens J. L. and Ron D. (1998) CHOP is implicated in programmed cell death in response to impaired function of the endoplasmic reticulum. *Genes Dev.* **12**, 982–995.

rich2/stm-stemc/stm-stemc/stm00106/stm0015d06a | smitherj | S=11 | 12/5/05 | 9:40 | 4/Color Figure(s): 1,4 | Art: SC-050124 | Input-??

STEM CELLS®
Tissue-Specific Stem Cells

AQ: 1

Activation of Canonical Wnt Pathway Promotes Proliferation of Retinal Stem Cells Derived From Adult Mouse Ciliary Margin

TOSHIHIRO INOUE,[a,b] TETSUSHI KAGAWA,[b,c] MIKIKO FUKUSHIMA,[a] TAKESHI SHIMIZU,[b] YUTAKA YOSHINAGA,[b] SHINJI TAKADA,[d] HIDENOBU TANIHARA,[a] TETSUYA TAGA[b]

[a]Department of Ophthalmology and Visual Science, Graduate School of Medical Sciences and [b]Department of Cell Fate Modulation, Institute of Molecular Embryology and Genetics, Kumamoto University Graduate School of Medical Science, Kumamoto, Japan; [c]Division of Active Transport, National Institute for Physiological Sciences, Okazaki, Japan; [d]Center for Integrative Bioscience, Okazaki National Research Institutes, Okazaki, Japan

AQ: 3

ABSTRACT

Fn1

Adult retinal stem cells represent a possible cell source for the treatment of retinal degeneration. However, only a small number of stem cells reside in the ciliary margin. The present study aimed to promote the proliferation of adult retinal stem cells via the Wnt signaling pathway. Ciliary margin cells from 8-week-old mice were dissociated and cultured to allow sphere colony formation. Wnt3a, a glycogen synthase kinase (GSK) 3 inhibitor, fibroblast growth factor (FGF) 2, and a FGF receptor inhibitor were then applied in the culture media. The primary spheres were dissociated to prepare either monolayer or secondary sphere cultures. Wnt3a increased the size of the primary spheres and the number of Ki-67–positive proliferating cells in monolayer culture. The Wnt3a-treated primary sphere cells were capable of self-renewal and gave rise to fourfold the number of secondary spheres compared with nontreated sphere cells. These cells also retained their multilineage potential to express several retinal markers under differentiating culture conditions. The Wnt3a-treated cells showed nuclear accumulation of β-catenin, and a GSK3 inhibitor, SB216763, mimicked the mitogenic activity of Wnt3a. The proliferative effect of SB216763 was attenuated by an FGF receptor inhibitor but was enhanced by FGF2, with Ki-67–positive cells reaching over 70% of the total cells. Wnt3a and SB216763 promoted the proliferation of retinal stem cells, and this was partly dependent on FGF2 signaling. A combination of Wnt and FGF signaling may provide a therapeutic strategy for in vitro expansion or in vivo activation of adult retinal stem cells. STEM CELLS *2006;0:000–000*

INTRODUCTION

The ciliary marginal zone is widely known to contain immature retinal cells that continue to divide throughout life in both amphibians and fish [1–7]. Recently, a limited number of ciliary margin cells in adult rodents were demonstrated to sustain stem cell characteristics in vitro [8, 9]. From a therapeutic viewpoint, stem cells residing in an adult tissue, if able to be expanded in vitro or activated in vivo, have a significant advantage in autologous transplantation or activation of endogenous stem cells because they can overcome immune rejection and the ethical concerns associated with using embryonic or neonatal tissues. Therefore, retinal stem cells in the adult ciliary margin have been highlighted as a possible cell source for stem cell therapies. However, it is debatable whether these cells can provide the copious stem cell pools required for therapy because a single primary sphere colony can only generate six to eight secondary

AQ: 2

Correspondence: ?. Received March 18, 2005; accepted for publication June 28, 2005. ©AlphaMed Press 1066-5099 doi: 10.1634/stemcells.2005-0124

spheres in the presence of fibroblast growth factor (FGF) 2 [9]. In addition, a limited number of primary spheres can be generated from individual adult eyes; only approximately 55 spheres were obtained from individual adult rodent eyes [9], and these spheres showed lower and restricted proliferation potential compared with neural stem cells derived from the adult subventricular zone [10]. Hence, improved and efficient strategies to expand retinal stem cells are required.

Wnt proteins are secreted lipid-modified signaling molecules that regulate cell proliferation and cell fate in various tissues in vertebrate embryos and can activate different intracellular signaling cascades, including the canonical pathway, c-Jun N-terminal kinase pathway, Ca^{2+} pathway, and focal adhesion kinase pathway (reviewed by Pandur et al. [11]). In the canonical pathway, Wnt protein binding to Frizzled (Fzd) and low-density lipoprotein receptor–related proteins (LRP) causes inactivation of glycogen synthase kinase (GSK) 3β and Axin, respectively. The inactivation of these proteins stabilizes β-catenin, which subsequently accumulates in the cell nucleus and activates the transduction of target genes that are crucial in the G1–S-phase transition, such as cyclin D1 or c-Myc (reviewed by Willert et al. [12]). Therefore, the canonical Wnt pathway contributes to cell proliferation in different types of stem cells [13–17].

During eye development in the chick, various components of Wnt signaling are expressed. Kubo et al. [18] demonstrated that Wnt2b can promote the proliferation of chick embryonic ciliary margin cells that can yield differentiated retinal progeny through activation of the canonical pathway. This finding encouraged us to explore whether Wnt signaling could promote the proliferation of adult retinal stem cells from the mammalian ciliary margin. In the present study, we demonstrate that Wnt3a increased the size of the spheres derived from ciliary margin. Wnt3a also increased the number of cells expressing Ki-67 and bromodeoxyuridine (BrdU) incorporation in triturated sphere cell cultures. More importantly, Wnt3a-treated sphere cells retained multipotency and formed a greater number of secondary spheres than nontreated cells, indicating that Wnt signaling functions on self-renewal of retinal stem cells (secondary sphere-forming ability). We further suggest that the Wnt3a-mediated increase in self-renewal involved the canonical pathway. Interestingly, the mitogenic effect of Wnt signaling was enhanced by exogenous FGF2 and attenuated by a FGF receptor inhibitor. Our results provide a basis for the development of useful strategies for the in vitro expansion of adult retinal stem cells.

Materials and Methods

Isolation and Culture

Eight-week-old C57Bl6 mice and green fluorescent protein (GFP) transgenic mice were used to prepare adult retinal stem cells as previously reported [9]. All studies were conducted in accordance with the guidelines of the Kumamoto University Center for Animal Resources and Development. Dissociated cells were cultured at clonal density for 5 days on six-well dishes (Nunc, Naperville, IL, http://www.nuncbrand.com) precoated with poly-HEME (Sigma-Aldrich, St. Louis, http://www.sigmaaldrich.com) in Dulbecco's modified Eagle's medium/F-12 medium (Invitrogen, Carlsbad, CA, http://www.invitrogen.com) containing B27 (Invitrogen) and various supplements: FGF2 (recombinant human FGF2; R&D Systems, Minneapolis, http://www.rndsystems.com), Wnt3a (recombinant mouse Wnt3a; catalog no. 1324-WN; R&D Systems), or SB216763 (Biomol Research Laboratories, Plymouth Meeting, PA, http://www.biomol.com). The cells were then triturated with enzymatic solution [9], replated on chamber slides (Nunc) precoated with poly-L-ornithine (Sigma-Aldrich) and fibronectin (Life Technologies, Gaithersburg, MD), and cultured for 2 days in B27/DMEM/F-12 containing various supplements: FGF2, Wnt3a, SB216763, Fzd-8-CRD (recombinant mouse Fzd-8/Fc chimera; R&D Systems), or SU5402 (EMD biosciences, San Diego, http://splash.emdbiosciences.com). The S-phase cells in these culture condition were further monitored by BrdU incorporation. After 2-day cultures with or without Wnt3a, the cells were pulse labeled with 10 μM BrdU for 4 hours, incubated in BrdU-free media for an additional 2 hours, and fixed for the immunochemical analyses. For secondary sphere formation, B27/DMEM/F-12 containing FGF2 and epidermal growth factor (EGF) (recombinant human EGF; R&D Systems) was used. To promote retinal cell differentiation, triturated cells were cultured for 7 days as previously described [9]. All cultures were maintained at 37°C in 5% CO_2.

Reverse Transcription–Polymerase Chain Reaction

Total RNA was isolated from sphere cells using Trizol (Invitrogen). Reverse transcription was performed on 2 μg of RNA using Superscript II (Invitrogen) according to the manufacturer's protocol. Reverse transcription products were amplified by polymerase chain reaction (PCR) using KOD-plus (Toyobo, Osaka, Japan, http://www.toyobo.co.jp) and gene-specific primers [19–22] under standard reaction conditions with an initial 2-minute denaturation step followed by 24 to 30 cycles of 94°C for 15 seconds, 58°C for 30 seconds, and 68°C for 60 seconds.

Immunocytochemistry

The cells were fixed with 4% paraformaldehyde for 10 minutes and then blocked with 3% goat serum in phosphate-buffered saline containing 0.1% Triton X-100 for 30 minutes. The cells were incubated for 2 hours with one or two of the following specific primary antibodies at the stated dilutions: mouse monoclonal anti–Ki-67 (1:200; BD Biosciences, Franklin Lakes, NJ,

http://www.bdbiosciences.com) as a cell-division marker; rat monoclonal anti-BrdU (1:40; Abcam, Cambridge, UK, http://www.abcam.com) as an S-phase cell marker; rabbit antiactive caspase-3 (1:200; BD Biosciences) as a cell-death marker; mouse monoclonal antirhodopsin (1:200; Chemicon International, Temecula, CA, http://www.chemicon.com/) as a rod photoreceptor cell marker; mouse monoclonal antisyntaxin (1:200; Sigma-Aldrich) and rabbit polyclonal anti-Pax6 (1:500; Chemicon International) as amacrine cell markers; mouse monoclonal antiglutamine (Gln) synthetase (1:200; Chemicon International) as a Müller glia marker; and mouse monoclonal anti-β-catenin (1:250; BD Biosciences). The cells were examined by epifluorescence after incubation for 30 minutes in Alexa 488- and/or Alexa 596-conjugated secondary antibodies (Molecular Probes, Eugene, OR; http://www.probes.com). Cell nuclei were counterstained with Hoechst 33258 (Nacalai Tesque, Kyoto, Japan, http://www.nacalai.co.jp). Negative controls were performed in parallel during all immunocytologic processing by omission of a primary antibody. No fluorescent labeling was observed in the negative controls. Images were obtained using an AX70 fluorescence microscope (Olympus, Tokyo, http://www.olympus-global.com) or TCS SP2 AOBS confocal microscope (Leica Microsystems, Wetzlar, Germany, http://www.leica-microsystems.com).

Statistical Analysis

The data represent the mean ± standard deviation of three separate experiments. For cytochemical studies, five randomly selected fields per sample were analyzed in each condition. Statistical significance was determined by Student's two-tailed *t*-test.

RESULTS

Stem Cell Properties of Ciliary Margin Cells

To ensure the existence of retinal stem cells from the ciliary margins of 8-week-old mice, the dissociated ciliary margin cells were cultured in the nonadherent condition at a clonal density. After 5 days in culture, sphere formation was observed. To further examine whether these sphere colonies were generated by the proliferation of single cells, ciliary margin cells were prepared from both GFP-expressing and wild-type mice, and the cell mixture was cultured at a clonal density for 5 days according to the method of Tropepe et al. [9]. Separate GFP-positive and GFP-negative spheres were observed (Fig. 1), demonstrating that the colonies were not derived from cell aggregation but instead arose clonally. Green spheres contained some dark dots, which might look like GFP-negative cells. However, they were not actually GFP-negative cells but differentiated pigment epithelial cells whose pigment may mask or impede the green color. These sphere cells were capable of generating secondary spheres and differentiating to express different retinal cell–specific markers, rhodopsin, syntaxin, and Pax6, under culture conditions that promoted retinal cell differentiation [8] (Table 1). Thus, the sphere cells from the ciliary margin possessed the stem cell characters of self-renewal and multilineage potential.

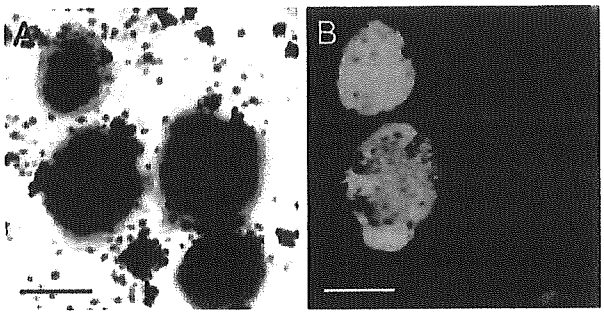

Figure 1. Clonal sphere formation of retinal stem cells from the adult ciliary margin. Phase **(A)** and fluorescence **(B)** photomicrographs are shown. Dissociated adult ciliary margin cells from GFP-expressing and wild-type mice were mixed and cultured in the nonadherent condition for 5 days. The mixture of dissociated cells generated distinctive spheres. Scale bars = 100 μm.

Effect of Wnt3a on Cell Proliferation

Because a limited number of primary spheres can be generated from individual adult eyes, improved and efficient strategies that expand the retinal stem cell pool by promoting cell proliferation are required. Wnt is a good candidate for this because it acts as a mitogen for immature retinal cells [18]. We first examined the expression of Wnt receptor genes in the sphere cells by reverse transcription–PCR. As shown in Figure 2A, gene products specific for Fzd-1, -3, -4, -6, -7, and -8 were amplified, whereas no signals for Fzd-2, -5, and -9 were detected. LRP-5 and -6, which are known to be indispensable receptors for the canonical Wnt pathway, were expressed. These results suggest that sphere cells from the adult ciliary

Table 1. Sphere cells expanded by Wnt3a or SB216763 retained their multilineage potential

	FGF2	Wnt3a	SB216763
Rhodopsin	10.2 ± 1.8	12.3 ± 2.4	10.6 ± 3.9
Syntaxin/Pax6	4.7 ± 1.2	3.9 ± 1.3	5.1 ± 0.2
Gln Synthetase	24.0 ± 5.6	24.0 ± 10.0	26.3 ± 10.4

The average percentage (± standard deviation) of cell types in the number of nuclei stained with Hoechst is shown in the column. Sphere colonies were grown in fibroblast growth factor 2 (FGF2)-, Wnt3a-, orSB216763-containing medium for 5 days. Thereafter, each sphere colony was plated and cultured for 21 days under conditions that promote retinal cell differentiation. The sphere-derived cells expressed several retinal cell–specific markers, such as rhodopsin as rod photoreceptors, Pax6 and syntaxin as amacrine cells, or Gln synthetase as Müller glia. In respect of these markers, any marked deviation of retinal cell fate was not observed among conditions of sphere formation.

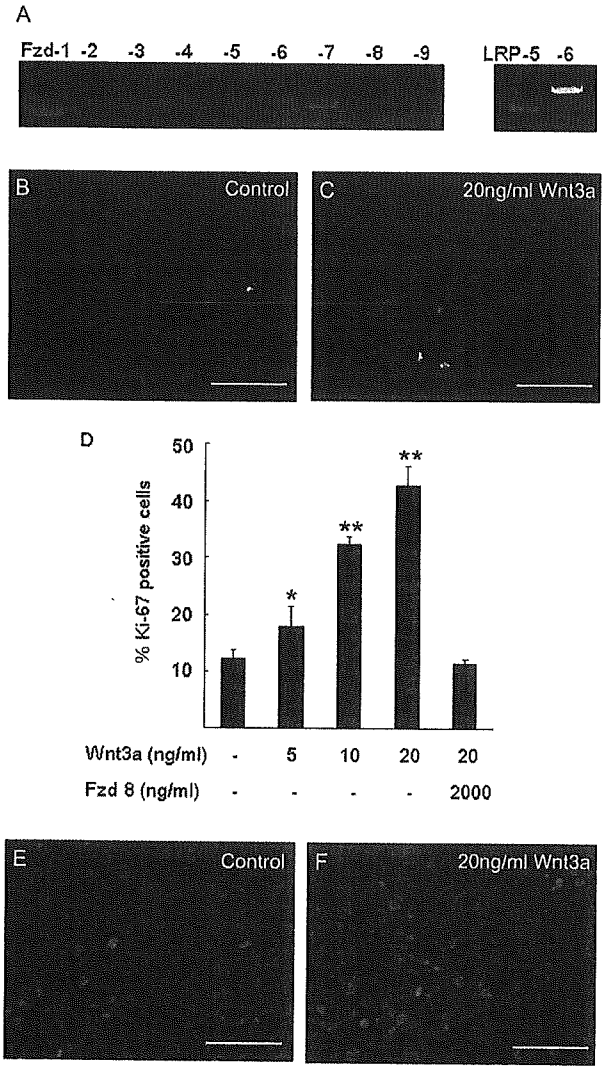

F3

Figure 2. Effect of Wnt3a on the cell-division markers. **(A):** Expression of Fzd family and LRP-5/6 mRNAs in the primary sphere cells were examined by reverse transcription–polymerase chain reaction. Gene products specific for Fzd-1, -3, -4, -6, -7, and -8 and LRP-5 and -6 were amplified. **(B–F):** Primary spheres were triturated and cultured in the adherent condition with various concentrations of Wnt3a for 48 hours. In the control cultures, 2.5 μg/ml dimethyl sulfoxide was added to the medium. The fluorescence photomicrographs **(B, C)** show merged images of Hoechst (blue) and anti–Ki-67 antibody (green) labeling. The number of Ki-67–positive cells in the culture containing 20 ng/ml Wnt3a **(C)** is greater than that in the control culture **(B)**. Quantification of Ki-67–positive cells **(D)** shows that Ki-67–positive cells increase in a Wnt3a dose-dependent manner, and Fzd-8-CRD (a Wnt antagonist) blocks this effect. All data represent the means ± standard deviations of three separate experiments. The fluorescence photomicrographs **(E, F)** show merged images of Hoechst (blue) and anti-bromodeoxyuridine (BrdU) antibody (red). In the presence of Wnt3a, the number of BrdU-incorporating cells is greater than that in the control condition. Scale bars = 100 μm. $*p < .05$, $**p < .01$ compared with control cultures.

margin have the prerequisites to react in response to Wnt proteins. To address the effect of Wnt signaling on the proliferation of adult retinal stem cells, the spheres were dissociated and cultured in the adherent condition for 48 hours in the presence of recombinant Wnt3a at a series of graded concentrations. The proliferative response was assayed by immunocytochemical staining for Ki-67, a cell-division marker [23]. Ki-67-positive cells were increased in a dose-dependent manner after the addition of Wnt3a (Figs. 2B–2D). This effect was maximal at 20 ng/ml Wnt3a, when the Ki-67-positive cells increased by 3.5-fold compared with control cultures. Since the recombinant Wnt3a used was only refined to 75% purity according to the manufacturer's description, there was a possibility that some of the impurities could have influenced the cell proliferation. Thus, Fzd-8-CRD, a Wnt antagonist [24, 25], was applied to the dissociation culture together with the recombinant Wnt3a. Sufficient dose of Fzd-8-CRD decreased the number of Ki-67–positive cells to the basal level (Fig. 2D), confirming the mitogenic effect of Wnt3a on sphere-derived cells. To examine DNA synthesis in the sphere-derived cells, they were pulse-labeled with BrdU for 4 hours. In the presence of 20 ng/ml Wnt3a, the number of BrdU-positive cells was increased from 10.2% ± 2.5% to 18.8% ± 1.6% ($p < .01$) (Figs. 2E, 2F), consistent with the increase in Ki-67–positive cells. Under all of the above conditions, there was no difference in the cell death estimated by immunocytochemical detection of activated caspase-3 (data not shown).

To further estimate the proliferative response, we assessed the size of the primary spheres (50 μm or more of the diameter) with or without Wnt3a. After a 5-day culture in vitro, the diameter of the spheres was increased in the presence of 20 ng/ml Wnt3a (Fig. 3A), consistent with the data in the adherent condition described above. Notably, the average volume of the Wnt3a-treated spheres was threefold larger than that of the control spheres, although various sizes of spheres appeared in Wnt3a-containing cultures. To exclude the possibility that Wnt3a increased each cell volume, the nuclei of sphere cells were stained by Hoechst 33258 and the cell densities were examined by the confocal microscope. The cell densities of the Wnt3a-treated spheres were nearly equal to those of control spheres (Figs. 3B, 3C), confirming that the size of the spheres was reflected in the cell number but not the cell size. On the contrary, there was no significant difference between the number of primary sphere colonies in the Wnt3a-containing and control cultures (data not shown), suggesting that Wnt3a did not affect the number of cells capable of forming primary spheres nor transform nonsphere forming cells into sphere-forming stem cells. Taken together, Wnt3a promotes the proliferation of sphere-forming cells from the adult ciliary margin.

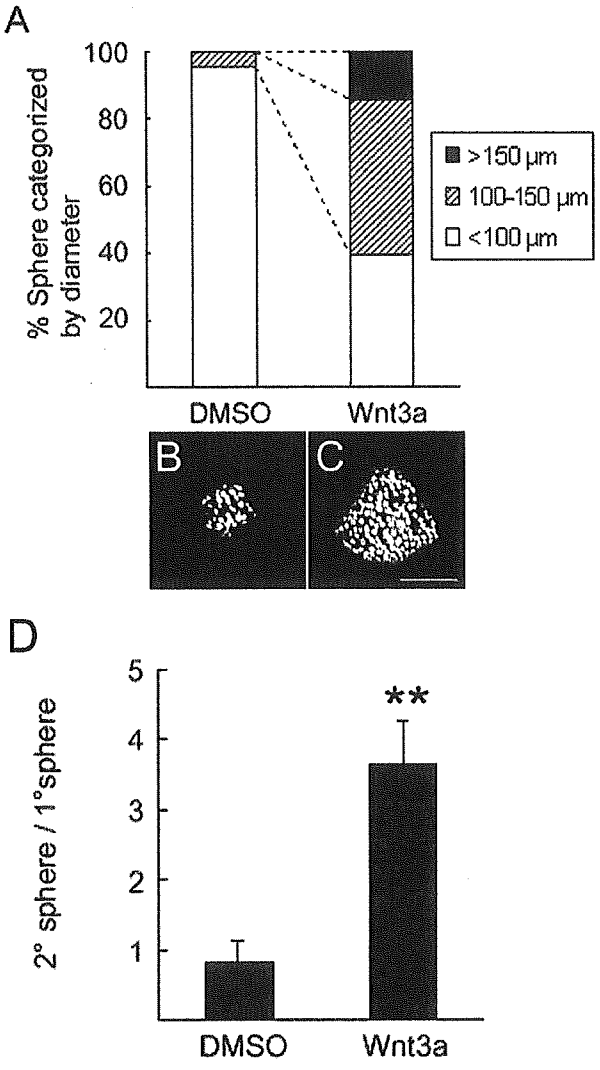

F4

Figure 3. Effect of Wnt3a on the sphere formation. **(A):** Percentages of spheres categorized by their diameter. Isolated ciliary margin cells were plated at 20,000 cells/ml and cultured in the nonadherent condition with 20 ng/ml Wnt3a for 5 days, and the sphere size was estimated. In the control cultures, 2.5 μg/ml dimethyl sulfoxide (DMSO) was added to the medium. A large proportion of spheres in the Wnt3a-containing culture are greater than 100 μm in diameter, whereas most of the spheres in the DMSO-treated control culture have diameters of 100 μm or less. The results are representative of three independent experiments. The percentages of sphere-forming cells with DMSO and Wnt3a were 0.098% ± 0.02% and 0.12% ± 0.03%, respectively. **(B,**

F5

C): Confocal microscopic images of the nuclei-counterstained primary spheres. The cell densities of the Wnt3a-induced large-sized spheres **(C)** were nearly equal to that of small-sized spheres in the control condition **(B)**. **(D):** Numbers of secondary spheres generated from primary spheres. Primary spheres were triturated and cultured in the nonadherent condition for 7 days in the presence of fibroblast growth factor 2 and epidermal growth factor. The number of secondary spheres generated from Wnt3a-treated spheres is greater than that from DMSO-treated control spheres. The results are the means ± standard deviations of three replicates. Scale bar = 100 μm. $^{**}p < .01$ compared with control cultures.

Characterization of Cells Expanded by Wnt3a

Although Wnt3a promoted the proliferation of sphere cells, it remained unclear whether this proliferation was accompanied by self-renewal of the adult retinal stem cells. If Wnt3a promoted self-renewal, the Wnt3a-treated cells should retain their stem cell characters even after proliferation. To test this hypothesis, individual primary sphere colonies cultured in the presence or absence of Wnt3a were dissociated and allowed to form secondary spheres. The Wnt3a-treated cells generated fourfold the number of secondary sphere colonies compared with dimethylsulfoxide (DMSO)-treated cells from a single primary sphere (Fig. 3D). In parallel with the increased sphere size after Wnt3a treatment, the Wnt3a-treated spheres contained greater numbers of stem cells than the control DMSO-treated spheres, indicating that Wnt 3a promotes proliferation of sphere-derived cells, including retinal stem cells.

To further characterize the cells expanded by Wnt3a, we next examined the multilineage potential of Wnt3a-treated cells. Sphere colonies grown in Wnt3a-containing medium were dissociated and cultured for 7 days under conditions that promote retinal cell differentiation as described above. The Wnt3a-treated cells expressed several retinal cell–specific markers, such as rhodopsin as rod photoreceptors (Fig. 4A), Pax6 and syntaxin as amacrine cells (Fig. 4B), or Gln synthetase as Müller glia (Fig. 4C). In respect of these markers, Wnt3a-treated cells did not show any marked deviation of retinal cell fate compared with FGF2-treated cells (Table 1). Thus, sphere cells expanded by Wnt3a retained their multilineage potential.

Activation of the Canonical Wnt Pathway

To investigate whether Wnt3a protein activates the canonical Wnt pathway in sphere-derived cells from the adult ciliary margin, we next examined the subcellular localization of β-catenin by immunocytochemistry. β-catenin is a coactivator of LEF/TCF-dependent transcription but is normally phosphorylated by GSK3β and quickly degraded. Activation of the canonical Wnt pathway inhibits the kinase activity of GSK3β, resulting in relocation of stabilized β-catenin to the nucleus. After trituration of primary spheres derived from the adult ciliary margin, the cells were cultured in the adhesive condition for 1 day and then treated with or without 20 ng/ml Wnt3a for 2 hours. The Wnt3a-treated cells showed nuclear accumulation of β-catenin (Fig. 5B, Wnt3a). In contrast, a low level of β-catenin was observed under the plasma membrane and in the cytoplasmic region of nontreated cells (Fig. 5A, control). Thus, Wnt3a is capable of activating the canonical Wnt pathway in sphere-derived cells.

Effect of a GSK3 Inhibitor on Proliferation

Despite the activation of the canonical pathway by Wnt3a, it remained unclear whether its activation was involved in pro-

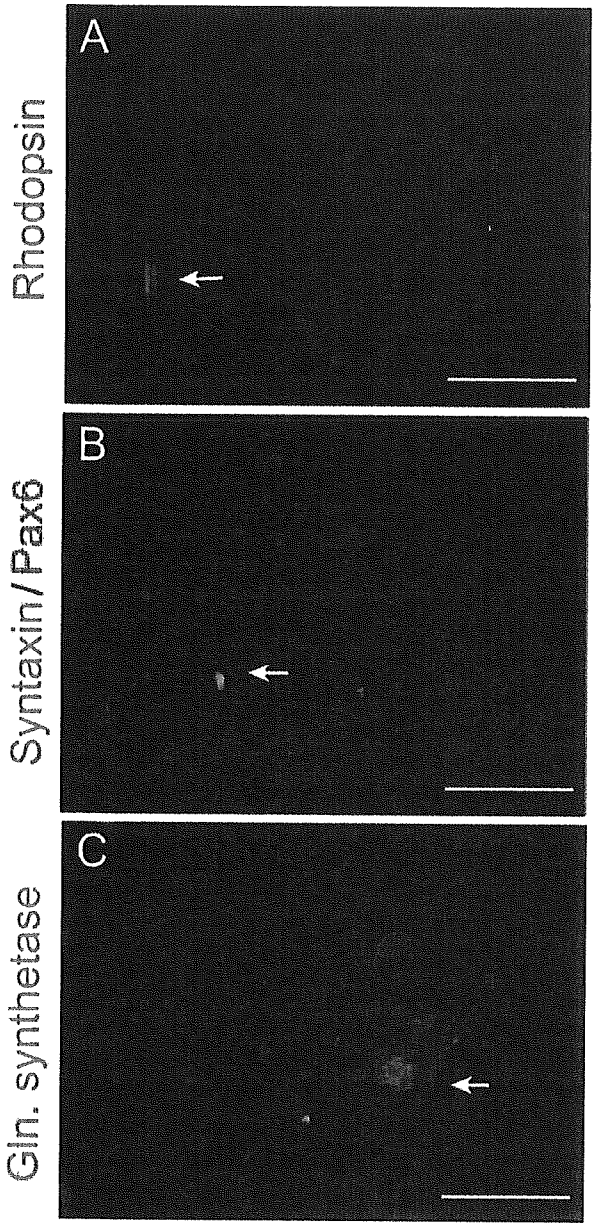

Figure 4. Fluorescence photomicrographs of differentiated cells. Wnt3a-treated sphere cells were triturated and cultured under conditions that promote retinal cell differentiation for 7 days. The Wnt3a-treated cells expressed several retinal cell–specific markers, such as rhodopsin as rod photoreceptors **(A)**, Pax6 and syntaxin as amacrine cells **(B)**, or glutamine (gln) synthetase as Müller glia **(C)**. Scale bars = 100 μm.

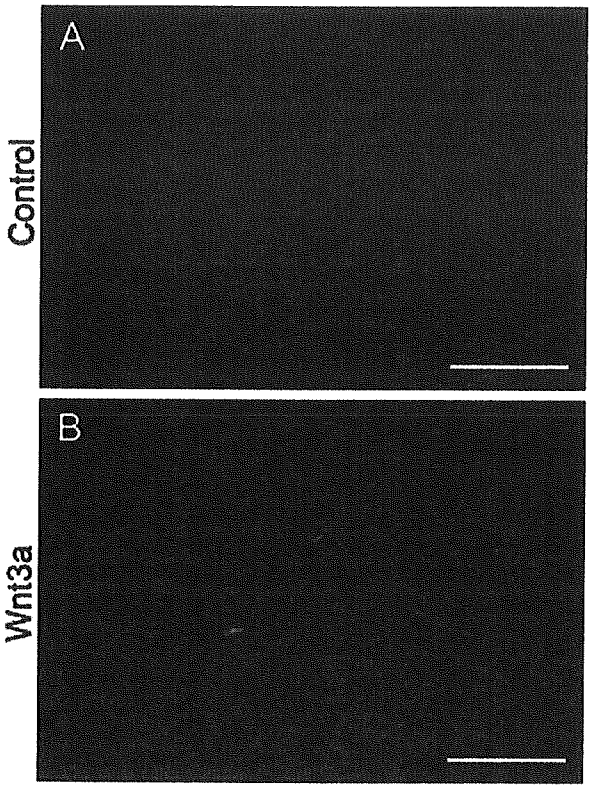

Figure 5. Nuclear translocation of β-catenin in the sphere-derived cells induced by Wnt3a. The localization of β-catenin was examined by immunohistochemistry at 2 hours after the addition of 2.5 μg/ml DMSO **(A)** or 20 ng/ml Wnt3a **(B)**. **(A):** β-catenin is observed in the cytoplasm and plasma membrane. **(B):** Wnt3a-treated cells show nuclear accumulation of β-catenin. Scale bars = 100 μm.

moting the proliferation of sphere-derived cells. Thus, we investigated the effect of SB216763, a specific GSK3 inhibitor [26]. GSK3β is a key enzyme in the canonical Wnt pathway that destabilizes β-catenin, and thus SB216763 addition is supposed to mimic Wnt3a stimulation [17, 27]. SB216763 treatment of sphere-derived cell cultures increased Ki-67–positive cells in a dose-dependent manner (Fig. 6A). This effect was maximal at 2.5 μM, when the number of Ki-67–positive cells increased by twofold compared with control cultures. Moreover, the sphere size was increased by SB216763 addition (Fig. 6B). Thus, the GSK3 inhibitor alone mimicked the Wnt3a activity on the proliferation of sphere-derived cells, suggesting that activation of the canonical Wnt pathway was involved in the enhancement of proliferation of sphere-derived cells. Moreover, the SB216763-treated cells expressed several retinal cell–specific markers under conditions that promote retinal cell differentiation and did not show any marked deviation of retinal cell fate compared with FGF2-treated cells (Table 1). Thus, sphere cells expanded by SB216763 retained their multilineage potential. F6

Cooperative Effect of FGF and Wnt Signaling

Adult retinal stem cells from the ciliary margin have been reported to release a small amount of endogenous FGF2 that promotes sphere formation since antibodies to FGF2 caused a reduction in the number of spheres [9]. To explore the effect of FGF2 on the canonical Wnt pathway, we used SU5402, a small

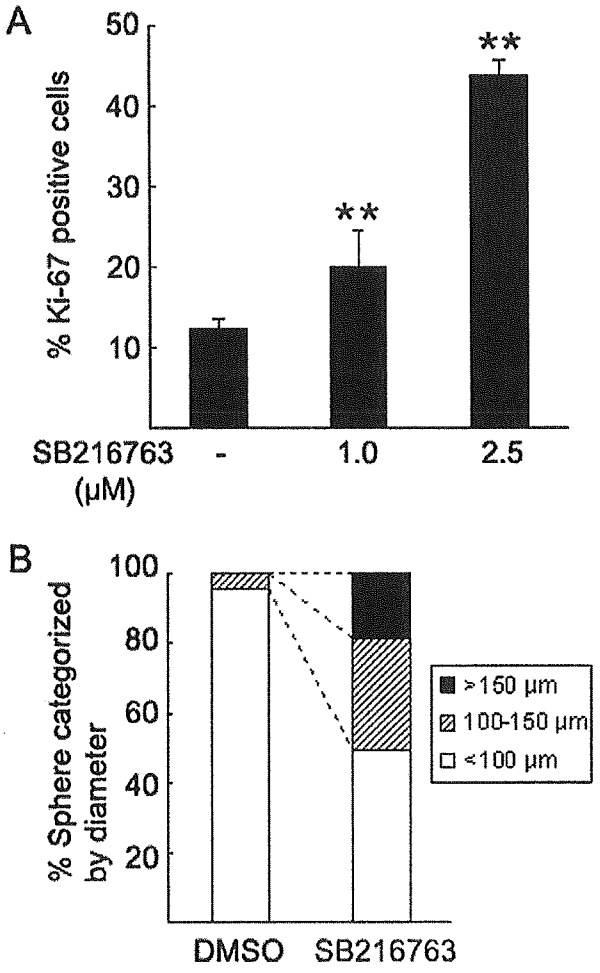

Figure 6. Increase in cell proliferation induced by SB216763 (a GSK3 inhibitor). **(A):** The percentage of Ki-67–positive cells was examined over the same time course described in the legend for Figure 2. The primary spheres were triturated and cultured in the adherent condition with SB216763 for 48 hours. Addition of 2.5 μM SB216763 increases the Ki-67-positive cells to 45% of the total cells. The results are the means ± standard deviations of three replicates. **p &λτ; 0.01 χομπαρεδ ωιτη χοντρολ χυλτυρεσ. Β) Τηε περχενταγεσ οφ τηε σπηερεσ ωερε χατεγοριζεδ βψ τηειρ διαμετερ ασ δεσχριβεδ ιν τηε λεγενδ φορ Φιγυρε 3. Α λαργε προπορτιον οφ σπηερεσ ιν τηε χυλτυρε χονταινινγ 2.5 μM SB216763 have diameters greater than 100 μm, whereas most spheres in the dimethylsulfoxide (DMSO)-treated control culture have diameters of 100 μm or less. The results are representative of three replicate experiments. The percentages of sphere-forming cells with DMSO and SB216763 were 0.098% ± 0.02% and 0.10% ± 0.01%, respectively.

AQ: 6

inhibitory molecule that is widely used to specifically interfere with signaling downstream of the FGF receptor (FGFR) [28]. Addition of FGF2 at 10 ng/ml to sphere-derived cell cultures increased the Ki-67–positive cells by threefold, and this activity was reduced to the control level by 6.0 μg/ml SU5402 (Fig. 7A). SU5402 decreased Ki-67–positive cells even in the absence of exogenous FGF2, supporting that endogenous FGF2 signaling was involved in the proliferation of retinal stem cells.

F7

We then added the FGFR inhibitor (SU5402) or FGF2 to the sphere-derived cell cultures in the presence of the GSK3 inhibitor (SB216763) and assessed the number of Ki-67–positive cells. Under all of the above conditions, there was no difference in the cell death estimated by immunocytochemical detection of activated caspase-3 (data not shown). Interestingly, the FGFR inhibitor attenuated the effect of the GSK3 inhibitor on cell proliferation and reduced the number of Ki-67–positive cells from 44%–18% (Fig. 7B). In contrast, exogenous FGF2 enhanced the proliferative effect of the GSK3 inhibitor and increased the Ki-67–positive cells to nearly 80% of the total cells, suggesting that there is an intense cooperative effect of FGF2 and Wnt signaling on cell proliferation of adult retinal sphere-derived cells.

Discussion

In the present study, we showed that Wnt3a increased the number of secondary spheres (promoting self-renewal) and that the expanded cells in the presence of Wnt3a preserved their stem cell abilities to yield differentiated progeny (maintaining multipotency), indicating that Wnt signaling has a mitogenic effect on adult retinal stem cells. It should be noted that sphere-derived cells may include retinal stem cells and committed retinal progenitor cells. Therefore, we refer to the sphere-derived cells as retinal stem/progenitor cells hereafter in this report. Wnt3a induced nuclear accumulation of β-catenin in retinal stem/progenitor cells. More strikingly, the GSK3 inhibitor SB216763, which can activate the canonical Wnt pathway, mimicked Wnt3a activity in terms of the enhancement of retinal stem/progenitor cell proliferation. These findings indicate that the canonical Wnt pathway contributes to the proliferative effect of Wnt3a on retinal stem/progenitor cells. Thus, our study provides evidence that activation of canonical Wnt signaling is useful for expanding retinal stem/progenitor cell pools in vitro. SB216763 is a less-expensive material than recombinant Wnt3a protein and could therefore reduce the cost of tissue engineering. Although the effect of another collateral pathway cannot be excluded, there is little evidence that noncanonical Wnt pathways positively regulate the cell cycle [11]. Although expression of Wnt3a was not detected in murine or avian eye [29, 30], we used commercially available recombinant Wnt3a to activate canonical Wnt pathway in this study. Recombinant Wnt3a was proved to induce self-renewal of hematopoietic stem cells by activation of canonical Wnt pathway [15], and activation of this pathway promotes proliferation of embryonic chick immature retinal cells [18].

Our study further suggests that the combination of FGF2 and Wnt3a has a strong additive effect on proliferation of adult retinal

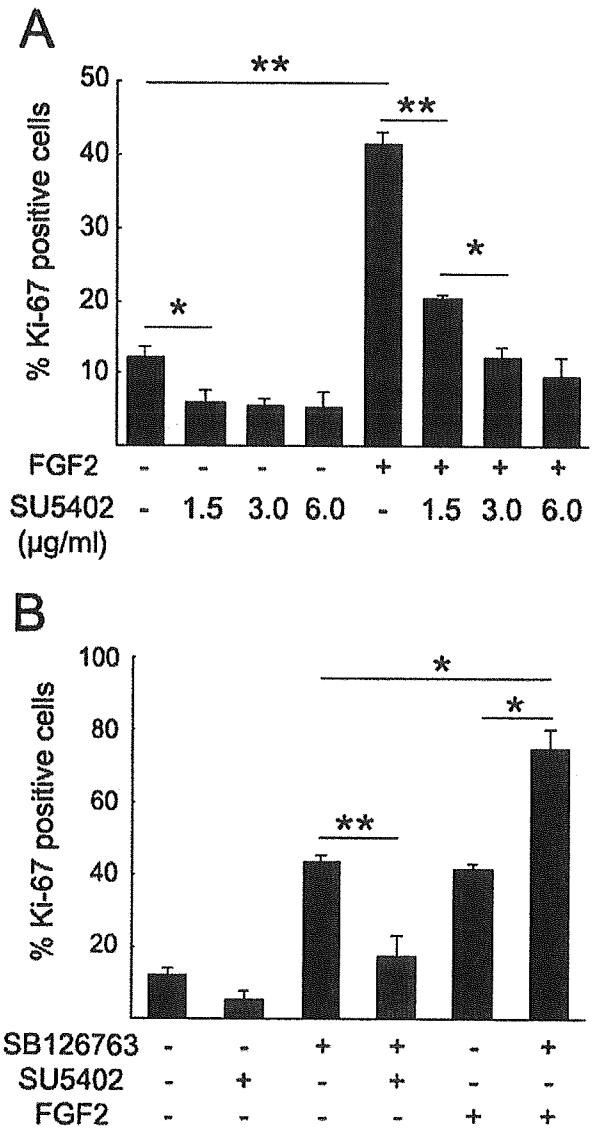

Figure 7. Effects of fibroblast growth factor 2 (FGF2) and its inhibitor on cell proliferation. The percentage of cells expressing Ki-67 was determined as described in the legend for Figure 2. Triturated sphere cells were cultured with FGF2, SU5402 (a FGF receptor inhibitor), SB216763, or their combination for 48 hours. **(A):** In the presence of exogenous FGF2, SU5402 decreases the Ki-67–positive cells in a dose-dependent manner. SU5402 decreases the Ki-67–positive cells, even in the absence of exogenous FGF2, suggesting the existence of endogenous FGF in the sphere-derived cell culture. **(B):** The effect of SB216763 on the cell proliferation is attenuated by SU5402 and enhanced by FGF2. The results are the means ± standard deviations of three replicates. $*p < .05$, $**p < .01$.

stem/progenitor cells. In the absence of endogenous FGF signaling, 7% of the total cells were Ki-67–positive. In the presence of the GSK3 inhibitor but without FGF signaling (after addition of the FGF receptor inhibitor), 18% of the total cells were Ki-67–positive (Fig. 7B). If the FGF-responsive and Wnt-responsive cells represent two different populations, 25% (7% + 18%) of the total cells should have been Ki-67–positive after the addition of the GSK3 inhibitor by itself. However, 44% of the cells were Ki67-positive, suggesting synergistic interaction between the FGF and Wnt signaling pathways. In other words, some of the retinal stem/progenitor cells showed cell cycle progression by activation of the canonical Wnt pathway that was dependent on endogenous FGF signaling. Concurrently with our present results, which we presented in the recent annual meeting of the Association for Research in Vision and Ophthalmology (Inoue T et al. , IOVS 2004;45: ARVO E-Abstract 5386), Das et al. independently showed that Wnt3a increased the number of primary spheres derived from an adult ciliary margin in the presence of FGF2 (Das AV et al. , IOVS 2004;45:ARVO E-Abstract 5396), supporting our data. AQ: 4 AQ: 5

As demonstrated in this study, the adult murine ciliary margin contains Wnt signal-responsive stem cells, although they are mitotically quiescent in vivo [31–34]. In addition, Wnt2b was reported to be expressed in the adult murine neural retina [29] and had the potential to induce proliferation of developing chick retinal precursors in vitro and in vivo via the canonical pathway [18]. The mechanism responsible for this difference between the in vivo and in vitro conditions remains unknown. N- and P-cadherin are expressed in the adult ciliary epithelium [35] and may contribute to attenuate cell proliferation by interference of the relocation of β-catenin into the nucleus (reviewed by Nelson et al. [36]). Secreted Wnt inhibitors, such as Sfrp family members expressed in the adult murine retina [29], also cannot be excluded because the roles of these molecules in the retina have not been well clarified. Another possibility is signal crosstalk with some other pathways, such as FGF signaling. The decreased FGF2 expression in the growing retina [37] could diminish the FGF-dependent proliferative effect of Wnt signaling. However, FGF2 may not actually be the partner of Wnt signaling in vivo because injured retinas were reported to express FGF2 but retinal regeneration by proliferation of retinal stem cells was not observed [38–41].

How can Wnt signaling be applied to stem cell therapy? It was recently reported that sphere cells generated from the ciliary margin could be incorporated into damaged or developing retinas, where they expressed retinal cell–specific markers, such as rhodopsin, syntaxin, and protein kinase C [42, 43]. Wnt signaling must be valuable for increasing the number of sphere colonies by continuous subcloning. Recently, Moshiri and Reh [44] reported that postnatal murine retinal margin cells showed a limited potential to regenerate retinal neurons using *patched* $(ptc)^{+/-}$ mice, in which Sonic hedgehog signaling is partially activated. In $ptc^{+/-}$ mice bred onto a retinal degeneration background, newly generated neurons and photoreceptors were observed at the retinal margin in vivo, similar to that in lower vertebrates. This observation suggests

the possibility that targeted manipulation of stem cells in the ciliary margin may lead to regeneration of damaged retinal neurons in higher vertebrates. If this is the case, the present results indicate that some molecules involved in the canonical Wnt pathway may be therapeutic targets. The effect of Wnt3a on the differentiation of the retinal stem cells derived from adult ciliary margin is not yet well clarified, and little is known about the crosstalk of Wnt signaling with the other mitotic factors for ciliary margin cells, such as insulin-like growth factor [45]. Further studies are required to fully characterize the proliferation and differentiation of retinal stem cells.

CONCLUSION

Wnt3a increased the self-renewal of retinal stem cells from the adult ciliary margin via the canonical pathway. A GSK3 inhibitor could mimic the proliferative effect of Wnt3a, which was partly dependent on FGF signaling. FGF and Wnt signaling showed a synergistic effect on retinal stem/progenitor cell proliferation, stimulating more than 75% of the total cells to become Ki-67–positive proliferating cells. These results may provide a novel therapeutic strategy for in vitro pooling or in vivo activation of retinal stem cells derived from the adult ciliary margin.

ACKNOWLEDGMENTS

The authors are very grateful to M. Ohta-Teramoto for secretarial assistance and to Y. Saiki for technical help. This work was supported by a Grant-in-Aid for 21st Century COE Research "Cell Fate Regulation Research and Education Unit" and Grant-in-Aid for Scientific Research (B) from the Ministry of Education, Culture, Sports, Science and Technology.

REFERENCES

1 Perron M, Kanekar S, Vetter ML et al. The genetic sequence of retinal development in the ciliary margin of the Xenopus eye. Dev Biol 1998; 199:185–200.

2 Wetts R, Serbedzija GN, Fraser SE. Cell lineage analysis reveals multipotent precursors in the ciliary margin of the frog retina. Dev Biol 1989;136:254–263.

3 Beach DH, Jacobson M. Patterns of cell proliferation in the retina of the clawed frog during development. J Comp Neurol 1979;183:603–613.

4 Meyer RL. Evidence from thymidine labeling for continuing growth of retina and tectum in juvenile goldfish. Exp Neurol 1978;59:99–111.

5 Johns PR. Growth of the adult goldfish eye, III: source of the new retinal cells. J Comp Neurol 1977;76:343–357.

6 Straznicky K, Gaze RM. The growth of the retina in Xenopus laevis: an autoradiographic study. J Embryol Exp Morphol 1971;26:67–79.

7 Hollyfield JG. Differential addition of cells to the retina in Rana pipiens tadpoles. Dev Biol 1968;18:163–179.

8 Ahmad I, Tang L, Pham H. Identification of neural progenitors in the adult mammalian eye. Biochem Biophys Res Commun 2000;270:517–521.

9 Tropepe V, Coles BL, Chiasson BJ et al. Retinal stem cells in the adult mammalian eye. Science 2000;287:2032–2036.

10 Engelhardt M, Wachs FP, Couillard-Despres S et al. The neurogenic competence of progenitors from the postnatal rat retina in vitro. Exp Eye Res 2004;78:1025–1036.

11 Pandur P, Maurus D, Kuhl M. Increasingly complex: new players enter the Wnt signaling network. Bioessays 2002;24:881–884.

12 Willert K, Nusse R. Beta-catenin: a key mediator of Wnt signaling. Curr Opin Genet Dev 1998;8:95–102.

13 van de Wetering M, Sancho E, Verweij C et al. The beta-catenin/TCF-4 complex imposes a crypt progenitor phenotype on colorectal cancer cells. Cell 2002;111:241–250.

14 Reya T, Duncan AW, Ailles L et al. A role for Wnt signalling in self-renewal of haematopoietic stem cells. Nature 2003;423:409–414.

15 Willert K, Brown JD, Danenberg E et al. Wnt proteins are lipid-modified and can act as stem cell growth factors. Nature 2003;423:448–452.

16 Liu BY, McDermott SP, Khwaja SS et al. The transforming activity of Wnt effectors correlates with their ability to induce the accumulation of mammary progenitor cells. Proc Natl Acad Sci U S A 2004;101:4158–4163.

17 Sato N, Meijer L, Skaltsounis L et al. Maintenance of pluripotency in human and mouse embryonic stem cells through activation of Wnt signaling by a pharmacological GSK-3-specific inhibitor. Nat Med 2004; 10:55–63.

18 Kubo F, Takeichi M, Nakagawa S. Wnt2b controls retinal cell differentiation at the ciliary marginal zone. Development 2003;130:587–598.

19 Hsieh M, Johnson MA, Greenberg NM et al. Regulated expression of Wnts and Frizzleds at specific stages of follicular development in the rodent ovary. Endocrinology 2002;143:898–908.

20 Heller RS, Dichmann DS, Jensen J et al. Expression patterns of Wnts, Frizzleds, sFRPs, and misexpression in transgenic mice suggesting a role for Wnts in pancreas and foregut pattern formation. Dev Dyn 2002;225: 260–270.

21 Tulac S, Nayak NR, Kao LC et al. Identification, characterization, and regulation of the canonical Wnt signaling pathway in human endometrium. J Clin Endocrinol Metab 2003;88:3860–3866.

22 Hoang BH, Kubo T, Healey JH et al. Expression of LDL receptor-related protein 5 (LRP5) as a novel marker for disease progression in high-grade osteosarcoma. Int J Cancer 2004;109:106–111.

23 Kee N, Sivalingam S, Boonstra R et al. The utility of Ki-67 and BrdU as proliferative markers of adult neurogenesis. J Neurosci Methods 2002; 115:97–105.

24 Hsieh JC, Rattner A, Smallwood PM et al. Biochemical characterization of Wnt-frizzled interactions using a soluble, biologically active vertebrate Wnt protein. Proc Natl Acad Sci U S A 1999;963546–3551.

25 Dann CE, Hsieh JC, Rattner A et al. Insights into Wnt binding and signalling from the structures of two Frizzled cysteine-rich domains. Nature 2001;412:86–90.

26 Cross DA, Culbert AA, Chalmers KA et al. Selective small-molecule inhibitors of glycogen synthase kinase-3 activity protect primary neurones from death. J Neurochem 2001;77:94–102.

27 Doble BW, Woodgett JR. GSK-3: tricks of the trade for a multi-tasking kinase. J Cell Sci 2003;116:1175–1186.

28 Mohammadi M, McMahon G, Sun L et al. Structures of the tyrosine kinase domain of fibroblast growth factor receptor in complex with inhibitors. Science 1997;276:955–960.

29 Liu H, Mohamed O, Dufort D et al. Characterization of Wnt signaling components and activation of the Wnt canonical pathway in the murine retina. Dev Dyn 2003;227:323–334.

30 Jin EJ, Burrus LW, Erickson CA. The expression patterns of Wnts and their antagonists during avian eye development. Mech Dev 2002;116: 173–176.

31 Cepko CL, Austin CP, Yang X et al. Cell fate determination in the vertebrate retina. Proc Natl Acad Sci U S A 1996;93:589–595.

32 Pittack C, Grunwald GB, Reh TA. Fibroblast growth factors are necessary for neural retina but not pigmented epithelium differentiation in chick embryos. Development 1997;124:805–816.

33 Feijen A, Goumans MJ, van den Eijnden-van Raaij AJ. Expression of activin subunits, activin receptors and follistatin in postimplantation mouse embryos suggests specific developmental functions for different activins. Development 1994;120:3621–3637.

34 Bodenstein L, Sidman RL. Growth and development of the mouse retinal pigment epithelium, I: cell and tissue morphometrics and topography of mitotic activity. Dev Biol 1987;121:192–204.

35 Xu L, Overbeek PA, Reneker LW. Systematic analysis of E-, N- and P-cadherin expression in mouse eye development. Exp Eye Res 2002;74: 753–760.

36 Nelson WJ, Nusse R. Convergence of Wnt, beta-catenin, and cadherin pathways. Science 2004;303:1483–1487.

37 Gao H, Hollyfield JG. Basic fibroblast growth factor in retinal development: differential levels of FGF2 expression and content in normal and retinal degeneration (rd) mutant mice. Dev Biol 1995;169:168–184.

38 Casson RJ, Chidlow G, Wood JP et al. The effect of retinal ganglion cell injury on light-induced photoreceptor degeneration. Invest Ophthalmol Vis Sci 2004;45:685–693.

39 Miyashiro M, Ogata N, Takahashi K et al. Expression of basic fibroblast growth factor and its receptor mRNA in retinal tissue following ischemic injury in the rat. Graefes Arch Clin Exp Ophthalmol 1998;236:295–300.

40 Cao W, Wen R, Li F et al. Mechanical injury increases bFGF and CNTF mRNA expression in the mouse retina. Exp Eye Res 1997;65:241–248.

41 Wen R, Song Y, Cheng T et al. Injury-induced upregulation of bFGF and CNTF mRNAS in the rat retina. J Neurosci 1995;15:7377–7385.

42 Chacko DM, Das AV, Zhao X et al. Transplantation of ocular stem cells: the role of injury in incorporation and differentiation of grafted cells in the retina. Vision Res 2003;43:937–946.

43 Coles BL, Angenieux B, Inoue T et al. Facile isolation and the characterization of human retinal stem cells. Proc Natl Acad Sci U S A 2004;101:15772–15777.

44 Moshiri A, Reh TA. Persistent progenitors at the retinal margin of $ptc^{+/-}$ mice. J Neurosci 2004;24:229–237.

45 Fischer AJ, Reh TA. Identification of a proliferating marginal zone of retinal progenitors in postnatal chickens. Dev Biol 2000;220:197–210.

Tissue Type Plasminogen Activator Facilitates NMDA-Receptor–Mediated Retinal Apoptosis through an Independent Fibrinolytic Cascade

Masako Kumada,[1,2] *Masayuki Niwa,*[1,3] *Akira Hara,*[4] *Hiroyuki Matsuno,*[1] *Hideki Mori,*[4] *Shigeru Ueshima,*[5] *Osamu Matsuo,*[5] *Tetsuya Yamamoto,*[2] *and Osamu Kozawa*[1]

Purpose. To investigate the association between apoptosis and the fibrinolytic system in retinal cell damage.

Methods. Tissue type plasminogen activator-deficient ($tPA^{-/-}$), urokinase type plasminogen activator-deficient ($uPA^{-/-}$), plasminogen activator inhibitor-1-deficient ($PAI\text{-}1^{-/-}$), $\alpha 2$ antiplasmin-deficient ($\alpha 2\ AP^{-/-}$) mice, and their wild-type counterparts were used. Retinal cell damage was induced by intravitreal injection of the excitotoxin *N*-methyl-D-aspartate (NMDA). The TdT-dUTP terminal nick-end labeling (TUNEL) method was used to examine retinal cell damage.

Results. $tPA^{-/-}$ mice were resistant to retinal cell damage caused by administration of NMDA, and $PAI\text{-}1^{-/-}$ mice were more injured than their wild-type. No significant difference was observed between $uPA^{-/-}$ or $\alpha 2\ AP^{-/-}$ and their wild-type mice.

Conclusions. The results strongly suggest that endogenous tPA, but not uPA acts as a facilitator in NMDA-induced retinal cell damage, and that its mechanism may not be associated with cleavage of plasminogen into plasmin in the fibrinolytic cascade. (*Invest Ophthalmol Vis Sci.* 2005;46:1504-1507) DOI:10.1167/iovs.04-0595

Tissue-type plasminogen activator (tPA) is used for the clinical treatment of thromboembolic stroke to activate the fibrinolytic system. The major source of tPA is endothelial cells; however, tPA has also been detected in neurons.[1] Therapeutic intervention with tPA in the nervous system may represent a two-edged sword, since it has been reported that tPA also promotes neurodegeneration after intracerebral injection of excitotoxins such as glutamate,[2] and neuronal damage after a cerebral infarction is thought to be mediated by excitotoxins.[3-6]

Retinal ganglion cell death is a common feature of many ophthalmic disorders, such as glaucoma and central artery or vein occlusion. Glaucoma in humans and monkeys is associated with a significant elevation in vitreal glutamate concentration.[7] The mechanism underlying retinal cell death in these diseases is not well understood. They are likely to involve, at least in part, ischemia-reperfusion injury, and the injury after ischemia may be due in part to the action of glutamate as an excitotoxin.[8]

Recently, we reported that tPA-deficient ($tPA^{-/-}$) mice are resistant to the retinal cell damage induced by excitotoxins, especially NMDA.[9] This result indicates that tPA facilitates NMDA-induced retinal cell damage, but the mechanism(s) by which tPA promotes retinal cell damage induced by NMDA, remains unclear.

The blood fibrinolytic system, which degrades intravascular fibrin, is activated by tPA or urokinase-type plasminogen activator (uPA), which convert plasminogen into plasmin.[10] These plasminogen activators are antagonized by an endogenous factor, plasminogen activator inhibitor-1 (PAI-1), and plasmin is inhibited by $\alpha 2$ antiplasmin ($\alpha 2$ AP).

In this study, to detect the association of excitotoxin-induced retinal cell death and the fibrinolytic system, $tPA^{-/-}$, uPA-deficient ($uPA^{-/-}$), PAI-1-deficient ($PAI\text{-}1^{-/-}$), and $\alpha 2$ AP-deficient ($\alpha 2\ AP^{-/-}$) mice and their wild-type counterparts were used. According to a method we previously described,[9] insult to the retina was delivered by intravitreal injection of NMDA, and the degree of neuronal damage was estimated by the TdT-dUTP terminal nick-end labeling (TUNEL) method.

Materials and Methods

Experiment Animals

Male $tPA^{-/-}$, $uPA^{-/-}$, $PAI\text{-}1^{-/-}$, $\alpha 2\ AP^{-/-}$, and wild-type mice weighing 25 to 30 g (on C57BL/6 and SV129 backgrounds) were used in the present study. Deficient mice were generated by homologous recombination in embryonic stem cells, as described previously.[11] All experiments were performed in accordance with the ARVO Statement for the Use of Animals in Ophthalmic and Vision Research.

Intravitreal Injection

Mice were anesthetized with intraperitoneal injections of 50 mg/kg pentobarbital sodium (Nembutal; Dainippon Pharmaceutical Co., Ltd., Osaka, Japan). According to the method we reported,[9] all animals were intravitreally injected with a 30-gauge needle 0.5 mm behind the limbus in the temporal region of the globe, through the conjunctiva and sclera. In animals with dilated pupils, it was possible to view the needle entering the vitreous. Both eyes of each mouse ($n = 6$–9) were routinely injected with 3 μL of 10 mM NMDA (30 nanomoles). The mice that had postoperative complications such as retinal hemorrhage, vitreous hemorrhage, and retinal detachment were excluded from the analysis.

Histology and TdT-dUTP Nick-End Labeling

The mice were killed with an overdose of pentobarbital sodium 12 hours after intravitreal injection. The eyes were enucleated and post-fixed overnight in phosphate-buffered 10% formalin and then embed-

From the Departments of [1]Pharmacology, [2]Ophthalmology, and [4]Tumor Pathology, and the [3]Medical Education Development Center, Gifu Graduate University School of Medicine, Gifu, Japan; and the [5]Department of Physiology, Kinki University School of Medicine, Osaka-Sayama, Japan.

Supported in part by a grant-in-aid for Scientific Research from the Ministry of Education, Science, Sports and Culture of Japan.

Submitted for publication May 26, 2004; revised September 29, 2004; accepted October 28, 2004.

Disclosure: **M. Kumada**, None; **M. Niwa** None; **A. Hara**, None; **H. Matsuno**, None; **H. Mori**, None; **S. Ueshima**, None; **O. Matsuo**, None; **T. Yamamoto**, None; **O. Kozawa**, None

The publication costs of this article were defrayed in part by page charge payment. This article must therefore be marked "*advertisement*" in accordance with 18 U.S.C. §1734 solely to indicate this fact.

Corresponding author: Masayuki Niwa, Department of Pharmacology and Medical Education Development Center, Gifu Graduate University School of Medicine, Yanagido, Gifu 501-1194, Japan; mniwa@cc.gifu-u.ac.jp.

Investigative Ophthalmology & Visual Science, April 2005, Vol. 46, No. 4